INFORMATION TO USERS

This was produced from a copy of a document sent to us for microfilming. While the most advanced technological means to photograph and reproduce this document have been used, the quality is heavily dependent upon the quality of the material submitted.

The following explanation of techniques is provided to help you understand markings or notations which may appear on this reproduction.

1. The sign or "target" for pages apparently lacking from the document photographed is "Missing Page(s)". If it was possible to obtain the missing page(s) or section, they are spliced into the film along with adjacent pages. This may have necessitated cutting through an image and duplicating adjacent pages to assure you of complete continuity.

2. When an image on the film is obliterated with a round black mark it is an indication that the film inspector noticed either blurred copy because of movement during exposure, or duplicate copy. Unless we meant to delete copyrighted materials that should not have been filmed, you will find a good image of the page in the adjacent frame.

3. When a map, drawing or chart, etc., is part of the material being photographed the photographer has followed a definite method in "sectioning" the material. It is customary to begin filming at the upper left hand corner of a large sheet and to continue from left to right in equal sections with small overlaps. If necessary, sectioning is continued again—beginning below the first row and continuing on until complete.

4. For any illustrations that cannot be reproduced satisfactorily by xerography, photographic prints can be purchased at additional cost and tipped into your xerographic copy. Requests can be made to our Dissertations Customer Services Department.

5. Some pages in any document may have indistinct print. In all cases we have filmed the best available copy.

University
Microfilms
International

300 N. ZEEB ROAD, ANN ARBOR, MI 48106
18 BEDFORD ROW, LONDON WC1R 4EJ, ENGLAND

HILL, ERIC VON KRUMREIG

THE VIBRATIONAL RESPONSE OF THE RECTANGULAR PARALLELEPIPED

The University of Oklahoma PH.D. 1980

PLEASE NOTE:

In all cases this material has been filmed in the best possible way from the available copy. Problems encountered with this document have been identified here with a check mark ✓.

1. Glossy photographs _____
2. Colored illustrations _____
3. Photographs with dark background _____
4. Illustrations are poor copy _____
5. Print shows through as there is text on both sides of page _____
6. Indistinct, broken or small print on several pages ✓
7. Tightly bound copy with print lost in spine _____
8. Computer printout pages with indistinct print _____
9. Page(s) _____ lacking when material received, and not available from school or author
10. Page(s) _____ seem to be missing in numbering only as text follows
11. Poor carbon copy _____
12. Not original copy, several pages with blurred type _____
13. Appendix pages are poor copy _____
14. Original copy with light type _____
15. Curling and wrinkled pages _____
16. Other _____

THE UNIVERSITY OF OKLAHOMA

GRADUATE COLLEGE

THE VIBRATIONAL RESPONSE OF THE RECTANGULAR PARALLELEPIPED

A DISSERTATION

SUBMITTED TO THE GRADUATE FACULTY

in partial fulfillment of the requirements for the

degree of

DOCTOR OF PHILOSOPHY

BY

ERIC von KRUMREIG HILL

Norman, Oklahoma

1980

THE VIBRATIONAL RESPONSE OF THE RECTANGULAR PARALLELEPIPED

APPROVED BY

Dan M. Egle

Akhtar S. Kham

J. N. Huffaker

L. W. White

C. W. Bert

DISSERTATION COMMITTEE

ACKNOWLEDGMENTS

I acknowledge first and foremost my Father in Heaven for inspiring me when I have worked for it and for loving me even when I have not. Much the same could be said for my wife, Marilynn, who is the finest woman I have ever met. She makes life worthwhile. I also give thanks to Dr. Davis M. Egle, my earthly source of inspiration, a man of great enthusiasm and humility and a lover of truth. Thanks must also go to Dr. Charles W. Bert for his immense storehouse of knowledge, to Dr. James N. Huffaker for his course, Mathematical Methods in Physics, and to Dr. Akhtar S. Khan and Dr. Luther W. White for their kindness and encouragement. Finally, I thank Mrs. Rose Benda for typing this dissertation and Mr. Brian Burrough for the art work. Their work speaks for itself.

ABSTRACT

This work presents exact normal mode solutions for the forced vibrational response of the rectangular parallelepiped with three sets of boundary conditions: (1) completely rigid-lubricated boundaries; (2) two stress-free and four rigid-lubricated boundaries; and (3) two elastically restrained and four rigid-lubricated boundaries. Both analytical and numerical verifications of these solutions are provided. Applications are discussed in the fields of acoustic emission non-destructive testing and the calibration of piezoelectric transducers.

TABLE OF CONTENTS

LIST OF FIGURES

LIST OF TABLES

CHAPTER I

INTRODUCTION

1.1 Background

The forced vibrational response of the rectangular parallelepiped is of particular interest in the study of wave propagation in solids and especially in the characterization of acoustic emission sources. Acoustic emission are the stress waves generated by the rapid release or redistribution of stored energy that accompany many deformation and fracture processes. The two major sources of acoustic emission are plastic deformation and crack growth. There has been considerable interest in studying the mechanisms associated with these sources in order to predict, and eventually perhaps control, flaw growth in structural materials.

Understanding the relationship between source and receiver in acoustic emission experiments has been the motivation for several recent papers [1-3] which have addressed the dynamic response of plates. However, many acoustic emission applications involve specimens of finite dimensions which are not accurately modeled by a plate. Some experimental work has been done on the source-receiver problem in finite bodies, but very little analytical work due mainly to the complexity of the mathematics describing the specimen response. In fact, there are no forced vibration solutions for parallelepipeds in the literature and only a few free vibration solutions [4-9,12-17].

It is the purpose of this work to help bridge the gap between the experimental and the analytical by providing normal mode solutions for the forced vibrational response of the rectangular parallelepiped with boundary conditions sufficiently realistic in a physical sense to allow inferences to be made concerning the source event. Obviously, the more realistic the boundary conditions, the more accurate the inferences. The two sets of boundary conditions considered here are (1) all six faces rigid-lubricated and (2) four rigid-lubricated and two stress-free faces. These represent approximations to the completely stress-free case, which has not, as yet, been solved by the classical normal mode technique. A third set of boundary conditions consisting of four rigid-lubricated and two elastically restrained faces is considered in Chapter IV. The solution to this problem is of interest because, by adjusting the value of the elastic modulus, the solutions for the previous two sets of boundary conditions can be recovered.

1.2 System Response

Much of what is known about the nature of acoustic emission sources has been learned through the use of piezoelectric transducers coupled to rectangular parallelepiped or plate type specimens. Unfortunately, by the time an acoustic emission signal is displayed on an output device, the waveform has undergone some very complex transformations. An example of these complexities is demonstrated in the simple crack growth monitoring system of Figure 1.1. Here, the specimen is under some type of loading which causes a material flaw to grow,

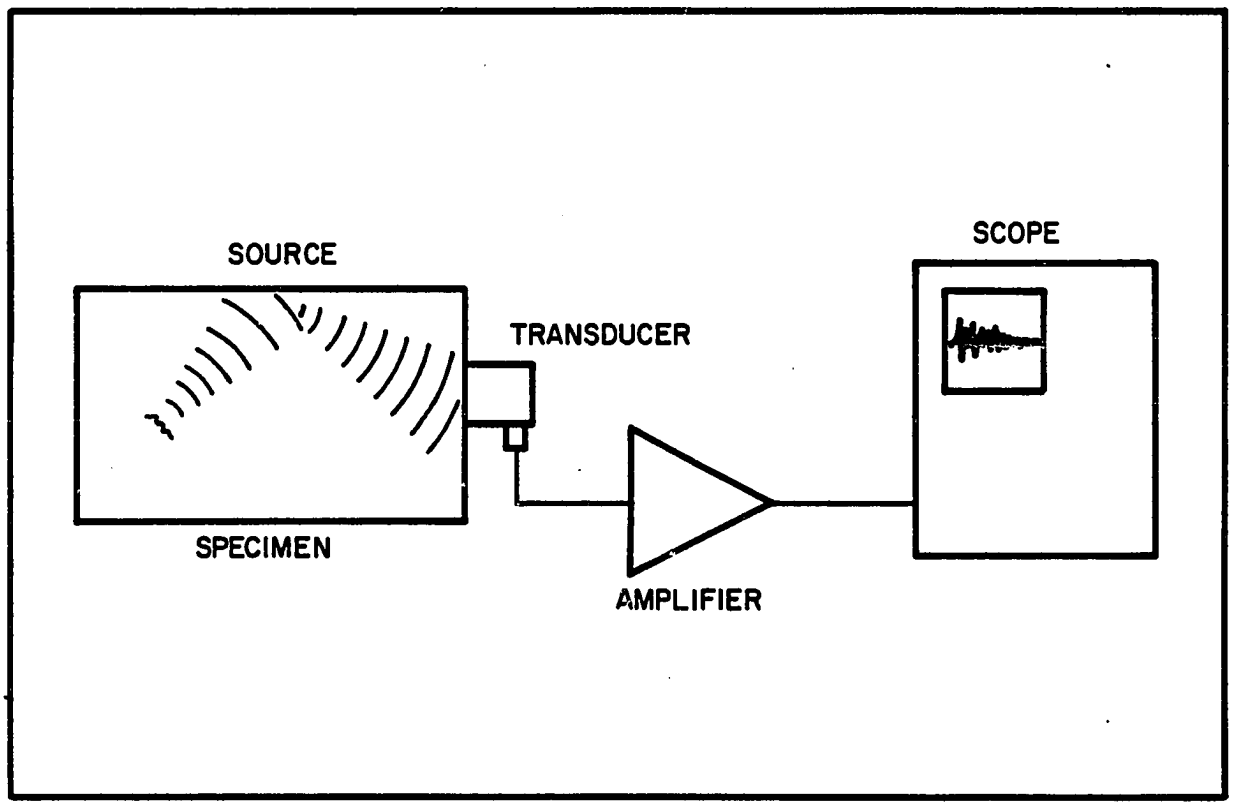

FIGURE 1.1
CRACK GROWTH MONITORING SYSTEM

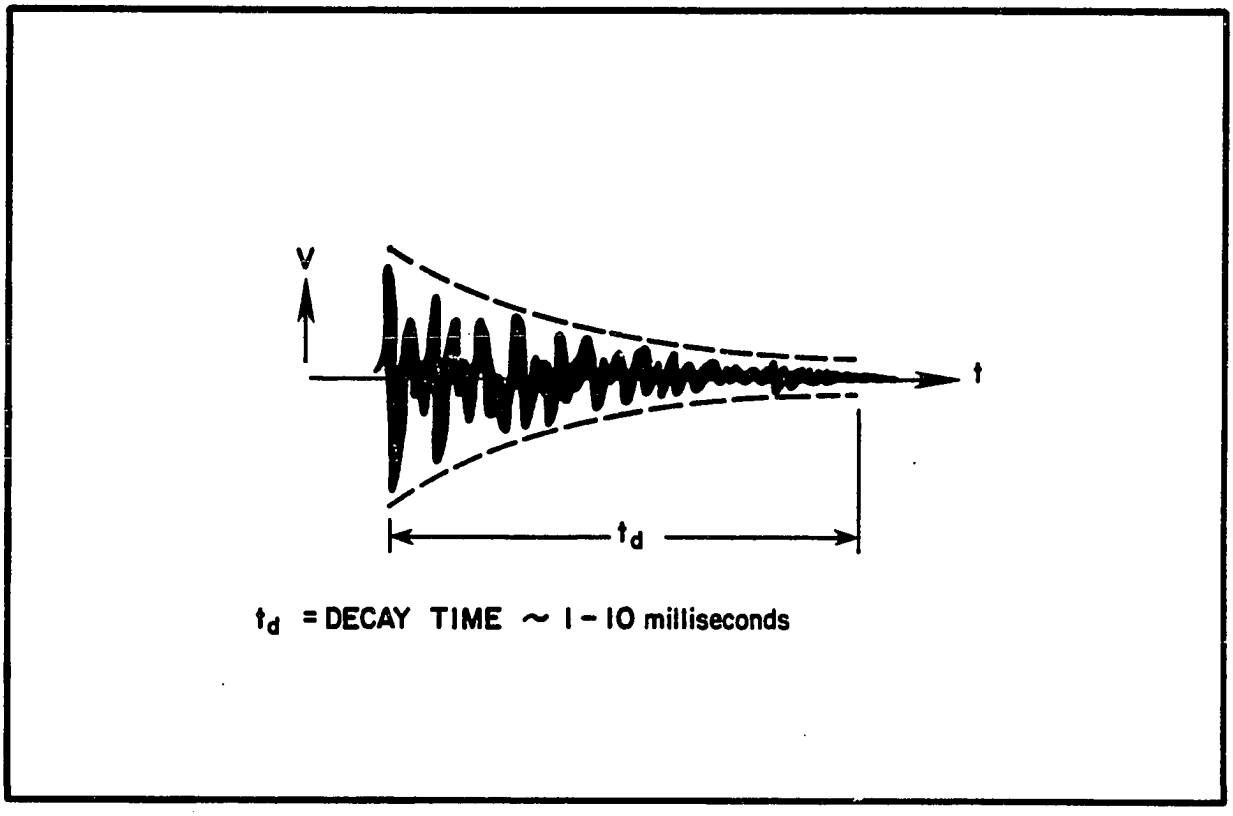

FIGURE 1.2

TYPICAL VOLTAGE VS TIME OSCILLOSCOPE DISPLAY
PRODUCED BY AN ACOUSTIC EMISSION BURST

thereby releasing energy in the form of acoustic emission. These waves reflect off the specimen boundaries and are sensed by the piezoelectric transducer. The piezoelectric crystal generates an electrical signal in proportion to the strength of the received stress wave. This signal is then amplified and displayed on an oscilloscope. A typical voltage versus time output trace for an acoustic emission burst is shown in Figure 1.2. Its attenuation is due primarily to damping at the specimen-transducer interface [7] and depends, to a much lesser extent, on the material properties.

Using a systems analysis approach, Spanner [8] postulated a linear response for the crack detection system as a whole; Houghton, Townsend and Packman [9] confirmed this experimentally. If it is assumed that the amplifier and the oscilloscope introduce no appreciable distortion to the transducer output, there are still three sources of distortion: the specimen, the specimen-transducer interface, and the transducer itself. The measured voltage response of the crack growth monitoring system as a function of frequency is then expressed as

$$H_{MEASURED}(\omega) = H_{TRANSDUCER/INTERFACE}(\omega)\, H_{SPECIMEN}(\omega)\, H_{SOURCE}(\omega), \quad (1.2.1)$$

where

$$H_{TRANSDUCER/INTERFACE}(\omega) = H_{TRANSDUCER}(\omega)\, H_{INTERFACE}(\omega)$$

is the combined transfer function for the transducer and the specimen-transducer interface.

To begin with, the only known quantity in equation (1.2.1) is $H_{MEASURED}(\omega)$. This is the frequency spectrum of the time-domain

oscilloscope output (Fig. 1.2) and can be measured experimentally. Given a known source and point of application, $H_{MEASURED}(\omega)$ may be calculated. For example, an impulse function has a uniform frequency spectrum from DC to 20 MHz; the frequency response of a step function decays exponentially. Then assuming that the transfer function for the specimen (specimen response) $H_{SPECIMEN}(\omega)$ can be determined, the transducer/interface response, $H_{TRANSDUCER/INTERFACE}(\omega)$ may be calculated according to equation (1.2.1), i.e., the transducer/interface can be calibrated. Once the transducer/interface is calibrated, the transfer function for any unknown source (of known location) can be obtained according to the expression

$$H_{SOURCE}(\omega) = \frac{H_{MEASURED}(\omega)}{H_{TRANSDUCER/INTERFACE}(\omega)\ H_{SPECIMEN}(\omega)}, \quad (1.2.2)$$

which is simply a rearrangement of equation (1.2.1). $H_{SOURCE}(\omega)$ can then be deconvoluted to obtain the time-domain source waveform. Inferences can then be made concerning the nature of the acoustic emission source and the mechanisms involved in its production.

Perhaps the system model which is the most physically realistic is a simply supported specimen with a uniform loading at the specimen-transducer interface and otherwise stress-free boundaries. One approximation to this system would be a specimen with completely stress-free boundaries. This approximate system is defined and discussed in the ensuing sections of this chapter along with two further simplifications of lesser mathematical difficulty.

1.3 Specimen Response

The specimen is assumed to be a homogeneous, isotropic, perfectly elastic solid. Its wave propagation is, therefore, governed by the linear three-dimensional theory of elastodynamics [10,11]. The coordinate system, dimensions, and stress convention are given in Figure 1.3, and the governing equation of motion is Navier's equation, which may be expressed in terms of wave speeds as

$$c_t^2 \nabla^2 \bar{u} + (c_\ell^2 - c_t^2) \nabla\nabla \cdot \bar{u} + \bar{f} = \frac{\partial^2 \bar{u}}{\partial t^2} \qquad (1.3.1)$$

with

$$\bar{u} = u_1 \hat{e}_1 + u_2 \hat{e}_2 + u_3 \hat{e}_3 = \text{displacement}$$

$$\bar{f} = f_1 \hat{e}_1 + f_2 \hat{e}_2 + f_3 \hat{e}_3 = \text{body force per unit mass}$$

$$u_i = u_i(x_1, x_2, x_3, t)$$

$$f_i = f_i(x_1, x_2, x_3, t) \qquad i=1,2,3 \ ;$$

$$\nabla = \frac{\partial}{\partial x_1} \hat{e}_1 + \frac{\partial}{\partial x_2} \hat{e}_2 + \frac{\partial}{\partial x_3} \hat{e} \ ;$$

and

$$c_\ell = \left[\frac{\lambda + 2\mu}{\rho}\right]^{\frac{1}{2}} = \text{longitudinal wave speed}$$

$$c_t = \left[\frac{\mu}{\rho}\right]^{\frac{1}{2}} = \text{transverse wave speed} \ .$$

Here, ρ is the density and λ and μ are the Lamé elastic constants. The body force term $\bar{f}$ is used to represent acoustic emission bursts. No surface forces are considered here since acoustic emission is primarily a body force phenomenon.

The boundary conditions for the completely stress-free rectangular parallelepiped are as follows:

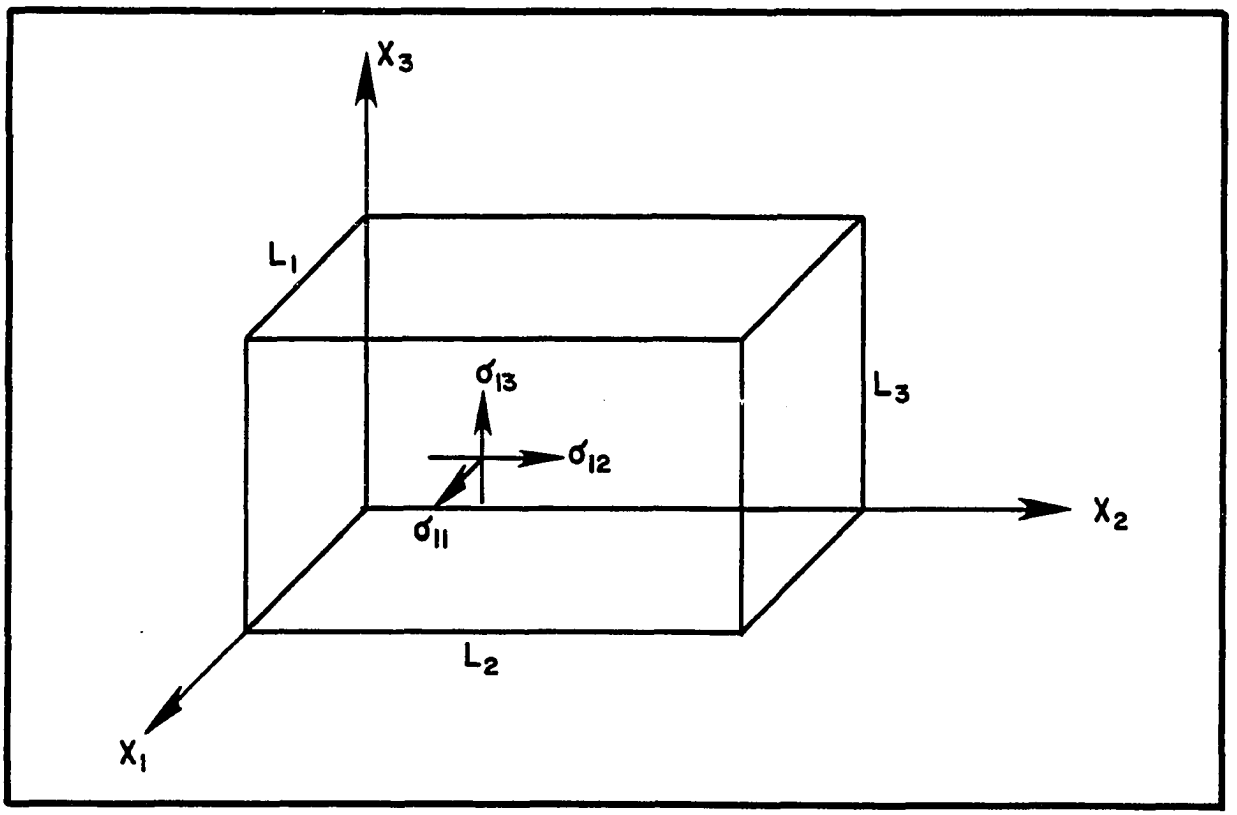

FIGURE 1.3
COORDINATE SYSTEM, DIMENSIONS AND STRESS CONVENTION

$$x_1 = 0, L_1 \qquad \sigma_{11} = \sigma_{12} = \sigma_{13} = 0$$

$$x_2 = 0, L_2 \qquad \sigma_{22} = \sigma_{21} = \sigma_{23} = 0$$

$$x_3 = 0, L_3 \qquad \sigma_{33} = \sigma_{31} = \sigma_{32} = 0 \ .$$

Writing the stresses in terms of displacements gives

$$\frac{\sigma_{11}}{\lambda} = \gamma \frac{\partial u_1}{\partial x_1} + \frac{\partial u_2}{\partial x_2} + \frac{\partial u_3}{\partial x_3}$$

$$\frac{\sigma_{22}}{\lambda} = \frac{\partial u_1}{\partial x_1} + \gamma \frac{\partial u_2}{\partial x_2} + \frac{\partial u_3}{\partial x_3}$$

$$\frac{\sigma_{33}}{\lambda} = \frac{\partial u_1}{\partial x_1} + \frac{\partial u_2}{\partial x_2} + \gamma \frac{\partial u_3}{\partial x_3}$$

$$\sigma_{12} = \sigma_{21} = \mu\left[\frac{\partial u_1}{\partial x_2} + \frac{\partial u_2}{\partial x_1}\right]$$

$$\sigma_{13} = \sigma_{31} = \mu\left[\frac{\partial u_1}{\partial x_3} + \frac{\partial u_3}{\partial x_1}\right]$$

$$\sigma_{23} = \sigma_{32} = \mu\left[\frac{\partial u_2}{\partial x_3} + \frac{\partial u_3}{\partial x_2}\right] ,$$

where $\gamma = 1 + \frac{2\mu}{\lambda}$. Therefore, the stress-free boundary conditions in terms of displacements become

$$\begin{aligned}
x_1 = 0, L_1 \quad & \gamma \frac{\partial u_1}{\partial x_1} + \frac{\partial u_2}{\partial x_2} + \frac{\partial u_3}{\partial x_3} = \frac{\partial u_1}{\partial x_2} + \frac{\partial u_2}{\partial x_1} = \frac{\partial u_1}{\partial x_3} + \frac{\partial u_3}{\partial x_1} = 0 \\
x_2 = 0, L_2 \quad & \frac{\partial u_1}{\partial x_1} + \gamma \frac{\partial u_2}{\partial x_2} + \frac{\partial u_3}{\partial x_3} = \frac{\partial u_2}{\partial x_1} + \frac{\partial u_1}{\partial x_2} = \frac{\partial u_2}{\partial x_3} + \frac{\partial u_3}{\partial x_2} = 0 \\
x_3 = 0, L_3 \quad & \frac{\partial u_1}{\partial x_1} + \frac{\partial u_2}{\partial x_2} + \gamma \frac{\partial u_3}{\partial x_1} = \frac{\partial u_3}{\partial x_1} + \frac{\partial u_1}{\partial x_3} = \frac{\partial u_3}{\partial x_2} + \frac{\partial u_2}{\partial x_3} = 0
\end{aligned} \qquad (1.3.2)$$

Within the parallelepiped there are two types of waves propagating, dilatational and equivoluminal, both of which are three-dimensional in nature. Any three-dimensional wave front, no matter what its shape, can be represented by an infinite set of contiguous points, each point

being the limiting case of a planar wave front. Accordingly, dilatational waves can be expressed in terms of an infinite sum of plane longitudinal waves propagating in every direction and equivoluminal waves in terms of a similar set of plane transverse waves; hence, the notation for the wave speeds, c_ℓ and c_t. These two wave types are depicted in Figure 1.4.

When either a longitudinal or a shear wave reflects off a stress-free surface, depending upon the angle of incidence, any one of three things can happen. The incident wave can either reflect unchanged; a portion of it can be mode converted into the other wave type, in which case two waves are reflected; or the incident wave can be entirely converted into a third wave type, the inhomogeneous wave. The most common type of inhomogeneous wave is the Rayleigh surface wave. These mode conversions at stress-free boundaries are only part of what make wave propagation problems in solids so difficult. The other part is the occurrence of multiple reflections between the boundaries in finite specimens.

The wave propagation problem can be simplified by assuming rigid-lubricated boundaries. This is because reflections from rigid-lubricated surfaces are specular, i.e., no mode conversions occur, only phase changes. Therefore, there are no inhomogeneous waves (imaginary wave numbers), and the only difficulty is multiple reflections. Physically, these boundary conditions suggest a problem in which a body is vibrating inside a container with infinitely rigid, frictionless walls. Although this is not representative of the typical acoustic emission experiment, the solution does provide a first step in solving

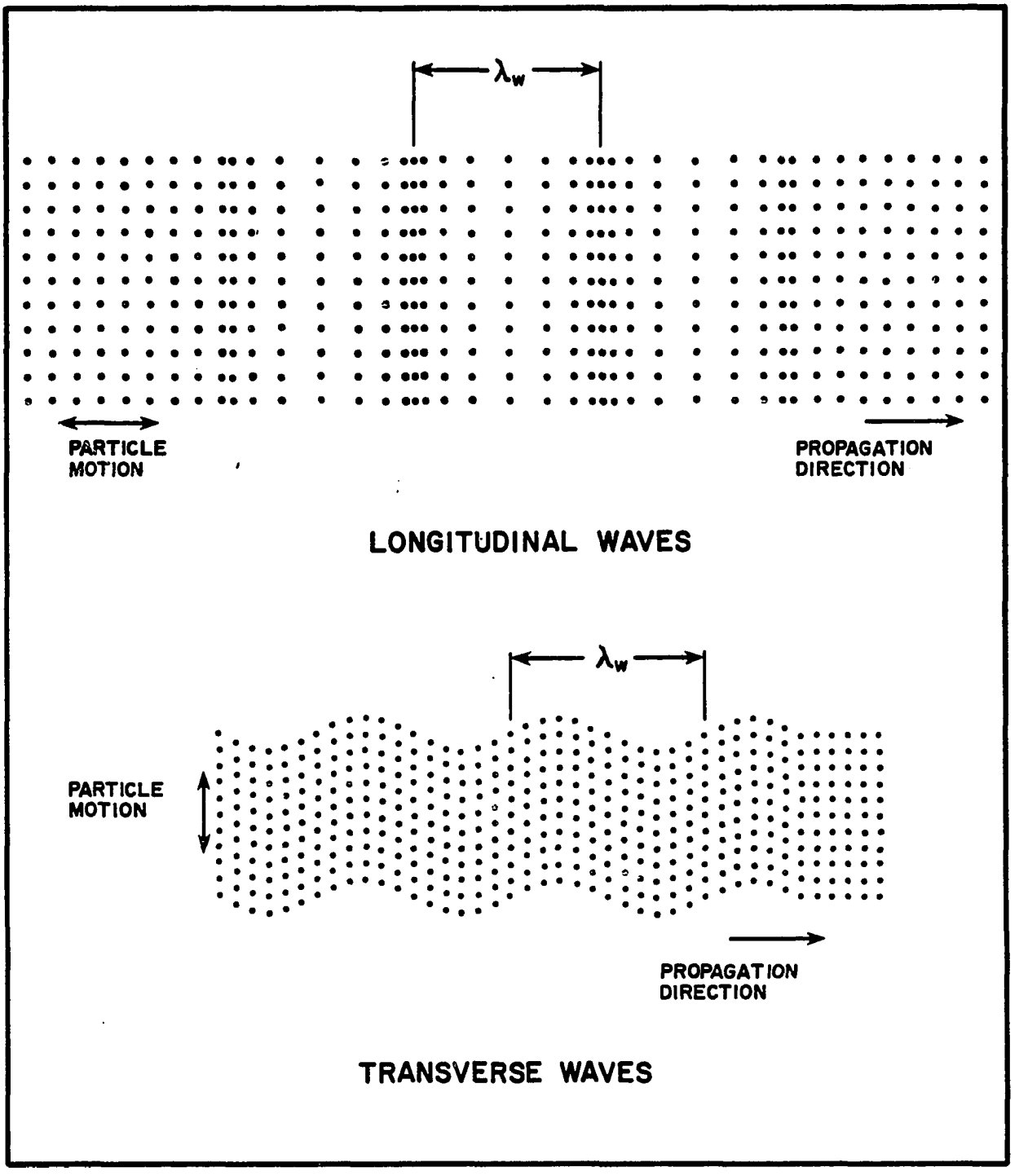

FIGURE 1.4
WAVES PROPAGATING WITHIN AN ELASTIC SOLID

for the more difficult stress-free cases.

Next in complexity is the solution for the problem of a rectangular parallelepiped with four rigid-lubricated and two stress-free boundaries. This problem is considerably more involved than the previous one due to the mode conversions on the two stress-free faces; on the other hand, it is also more realistic. Here, there are longitudinal-shear and shear-longitudinal conversions corresponding to the real wave numbers and shear-inhomogeneous conversions associated with the imaginary wave numbers, and as before, there are multiple reflections.

The problem of the parallelepiped with completely stress-free boundaries is the most complex of the three presented and also the most realistic. It allows for mode conversions at all the boundaries as well as multiple reflections. The next section discusses normal mode solutions to these three problems.

1.4 Normal Mode Solutions

The normal mode technique is appropriate for solving vibration or wave propagation problems in finite bodies. This is true because finite bodies only vibrate at discrete frequencies as opposed to infinite bodies which respond to the whole frequency spectrum. The displacement pattern associated with each of the natural frequencies is called a normal mode, and all the normal modes combine to give the total vibration or displacement pattern of the body. Separation of variables is the approach typically used to determine the natural frequencies and normal modes of a given system.

In order to solve for the forced vibrational response of any system using the normal mode approach, it is necessary to first solve for the free vibrational response. The free vibration problem for a rectangular parallelepiped with rigid-lubricated boundaries was first solved by Ortway [4] in 1913 and repeated by Nadeau [5] in 1964. In an effort to preserve continuity, Nadeau's solution is recast in Chapter II. The forced vibration problem is solved by first uncoupling the equations of motion using a vector displacement function, then utilizing a normal mode approach to obtain the desired displacements.

The free vibration solution for the case of four rigid-lubricated and two stress-free boundaries is the work of Kaliski as presented by Malecki [12]. Kaliski's original work [13] is in Polish; Malecki's text provides an English translation. Several significant errors were discovered in this presentation. As such, the free vibration problem is reworked in its entirety in Chapter III. This includes many of the details omitted by Malecki. The forced vibration problem is then solved by the normal mode technique.

Using a straightforward normal mode approach to solve the problem of the rectangular parallelepiped with completely stress-free boundaries, one obtains trivial solutions only. This is because separation of variables assumes factored solutions of the form

$$u_i(x_1,x_2,x_3,t) = X_{1i}(x_1)X_{2i}(x_2)X_{3i}(x_3)T(t), \quad i=1,2,3 \qquad (1.4.1)$$

and no member of this set can satisfy the completely stress-free boundary conditions. In fact, the use of such solutions leads to the situation where there are more equations than unknowns.

The additional unknowns can be generated systematically using the method of associated periodicity developed by Fromme and Leissa [14,15]. They applied this technique to obtain a periodic extension of Navier's equation (1.2.1) and the stress-free boundary conditions and then employed Fourier analysis to reduce the partial differential equations to a set of algebraic equations. These equations were then solved to obtain the complete eigenspectrum for the free vibration problem. One significant drawback to this technique is the need to solve an infinite matrix in order to determine the natural frequencies.

Budanov and Orlov [16] obtained a portion of the eigenspectrum by assuming a particular form for $\nabla\cdot\bar{u}$ and solving for the symmetric modes. The antisymmetric modes were not considered, nor were any other forms for $\nabla\cdot\bar{u}$; moreover, several simplifying approximations were made in their numerical computations. In spite of all this, their computed natural frequencies for the rigid body modes did compare favorably with experimental beam data. There was no indication as to how well this analysis worked on rectangular parallelepipeds having dimensions of similar magnitude.

The two solutions discussed above are the only known exact analytical solutions for the free vibrational response of the rectangular parallelepiped with stress-free boundaries. Both of them are algebraically very complex, which may explain why neither work has been referenced in any recent publications. Because of this complexity, and the need for a forced vibration solution to model acoustic emission activity, the author made several attempts to solve this problem using other approaches. Unfortunately, none of them were successful. As a

consequence, the solution developed herein for the forced vibration of the rectangular parallelepiped with four rigid-lubricated and two stress-free boundaries probably represents the best available analytical tool to model acoustic emission activity in parallelepipeds with stress-free boundaries. The completely rigid-lubricated problem mainly provides a first step in obtaining the more difficult rigid-lubricated/stress-free solution.

CHAPTER II

RIGID-LUBRICATED BOUNDARIES

2.1 Free Vibration Solution

The equations of motion for the free vibration solution are Navier's equations (1.3.1) with the body force terms set equal to zero:

$$c_t^2\nabla^2\bar{u} + (c_\ell^2 - c_t^2)\nabla\nabla\cdot\bar{u} = \frac{\partial^2\bar{u}}{\partial t^2} \ . \tag{2.1.1}$$

The rigid-lubricated boundary conditions are given as

$$\begin{aligned} x_1 = 0,L_1 \qquad & u_1 = 0 \qquad \sigma_{12} = \sigma_{13} = 0 \\ x_2 = 0,L_2 \qquad & u_2 = 0 \qquad \sigma_{21} = \sigma_{23} = 0 \\ x_3 = 0,L_3 \qquad & u_3 = 0 \qquad \sigma_{31} = \sigma_{32} = 0 \ , \end{aligned}$$

which, in terms of displacements, become

$$\begin{aligned} x_1 = 0,L_1 \qquad & u_1 = 0 \qquad \frac{\partial u_2}{\partial x_1} = \frac{\partial u_3}{\partial x_1} = 0 \\ x_2 = 0,L_2 \qquad & u_2 = 0 \qquad \frac{\partial u_1}{\partial x_2} = \frac{\partial u_3}{\partial x_2} = 0 \\ x_3 = 0,L_3 \qquad & u_3 = 0 \qquad \frac{\partial u_1}{\partial x_3} = \frac{\partial u_2}{\partial x_3} = 0 \end{aligned} \tag{2.1.2}$$

The problem may be solved by assuming simple harmonic motion of the parallelepiped and normal mode displacement components of the form [4-6]

$$u_{1N} = A_{1N} \sin k_1 x_1 \cos k_2 x_2 \cos k_3 x_3 \sin\omega_N t$$

$$u_{2N} = A_{2N} \cos k_1 x_1 \sin k_2 x_2 \cos k_3 x_3 \sin \omega_N t \qquad (2.1.3)$$

$$u_{3N} = A_{3N} \cos k_1 x_1 \cos k_2 x_2 \sin k_3 x_3 \sin \omega_N t \ ,$$

where the ω_N are the natural frequencies or eigenvalues of the system. In order to satisfy the boundary conditions, the wave numbers must be $k_1 = n_1\Pi/L_1$, $k_2 = n_2\Pi/L_2$, and $k_3 = n_3\Pi/L_3$ with n_1, n_2, n_3 being the integers from zero to infinity. The direction of propagation of each component wave is determined by the set of integer indices $N(n_1,n_2,n_3)$. Substituting the above assumed normal modes into the equations of motion (2.1.1), one obtains for each set N,

$$\begin{bmatrix} \beta_N + k_1^2 & k_1k_2 & k_1k_3 \\ k_1k_2 & \beta_N + k_2^2 & k_2k_3 \\ k_1k_3 & k_2k_3 & \beta_N + k_3^2 \end{bmatrix} \begin{Bmatrix} A_{1N} \\ A_{2N} \\ A_{3N} \end{Bmatrix} = 0 \qquad (2.1.4)$$

with $\beta_N = (c_t^2\alpha_N^2 - \omega_N^2)/(c_\ell^2 - c_t^2)$ and $\alpha_N^2 = k_1^2 + k_2^2 + k_3^2$. This set of equations has a nontrivial solution if and only if the determinent of the 3x3 matrix is equal to zero, i.e.,

$$(\beta_N + \alpha_N^2)\beta_N^2 = 0 \ . \qquad (2.1.5)$$

Equation (2.1.5) is the characteristic equation. Corresponding to its roots, $\beta_{1N} = -\alpha_N^2$ and $\beta_{2N}=\beta_{3N}=0$, are the natural frequencies of the system

$$\omega_{1N} = c_\ell \alpha_N \qquad (2.1.6)$$

$$\omega_{2N} = \omega_{3N} = c_t \alpha_N \ . \qquad (2.1.7)$$

It can be shown [11,14] that ω_{1N} is associated with dilatational waves and $\omega_{2N}=\omega_{3N}$ with the two orthogonal polarizations of equivoluminal

waves. Thus, each displacement component (u_1,u_2,u_3) is made up of three contributions, one due to dilatational waves and the other two due to equivoluminal waves. However, as was mentioned previously, any three-dimensional wave front can be expressed in terms of infinite sums of plane longitudinal and transverse wave components so that $\omega_{1N}=\omega_{\ell N}$ and $\omega_{2N}=\omega_{3N}=\omega_{tN}$, and therefore

$$
\begin{aligned}
u_1 &= \sum_N \sin k_1 x_1 \cos k_2 x_2 \cos k_3 x_3 \left[(A_{1N})_\ell \sin\omega_{\ell N} t + (A_{1N})_t \sin\omega_{tN} t\right] \\
u_2 &= \sum_N \cos k_1 x_1 \sin k_2 x_2 \cos k_3 x_3 \left[(A_{2N})_\ell \sin\omega_{\ell N} t + (A_{2N})_t \sin\omega_{tN} t\right] \qquad (2.1.8) \\
u_3 &= \sum_N \cos k_1 x_1 \cos k_2 x_2 \sin k_3 x_3 \left[(A_{3N})_\ell \sin\omega_{\ell N} t + (A_{3N})_t \sin\omega_{tN} t\right] ,
\end{aligned}
$$

with the notation $\sum_N = \sum_{n_1=0}^{\infty} \sum_{n_2=0}^{\infty} \sum_{n_3=0}^{\infty}$.

The longitudinal wave amplitude relations are determined by substituting $\omega_N=\omega_{\ell N}$ back into equation (2.1.4). This gives the result

$$
\begin{aligned}
(A_{1N})_\ell &= (A_{1N})_\ell \\
(A_{2N})_\ell &= \frac{k_2}{k_1} (A_{1N})_\ell \qquad (2.1.9) \\
(A_{3N})_\ell &= \frac{k_3}{k_1} (A_{1N})_\ell .
\end{aligned}
$$

A similar procedure determines the amplitude relations for the transverse waves:

$$
\begin{aligned}
(A_{1N})_t &= (A_{1N})_t \\
(A_{2N})_t &= (A_{2N})_t \qquad (2.1.10) \\
(A_{3N})_t &= -\frac{k_1}{k_3} (A_{1N})_t - \frac{k_2}{k_3} (A_{2N})_t .
\end{aligned}
$$

Thus, displacements (2.1.8) become

$$
\begin{aligned}
u_1 &= \sum_N \sin k_1 x_1 \cos k_2 x_2 \cos k_3 x_3 \{(A_{1N})_\ell \sin\omega_{\ell N} t + (A_{1N})_t \sin\omega_{tN} t\} \\
u_2 &= \sum_N \cos k_1 x_1 \sin k_2 x_2 \cos k_3 x_3 \{\frac{k_2}{k_1}(A_{1N})_\ell \sin\omega_{\ell N} t + (A_{2N})_t \sin\omega_{tN} t\} \\
u_3 &= \sum_N \cos k_1 x_1 \cos k_2 x_2 \sin k_3 x_3 \{\frac{k_3}{k_1}(A_{1N})_\ell \sin\omega_{\ell N} t \\
&\qquad - [\frac{k_1}{k_3}(A_{1N})_t + \frac{k_2}{k_3}(A_{2N})_t]\sin\omega_{tN} t\} \ .
\end{aligned}
\tag{2.1.11}
$$

These equations represent the free vibration displacements of any point within or on the surface of the rectangular parallelepiped as a function of time. The displacements $(A_{1N})_\ell$, $(A_{1N})_t$, and $(A_{2N})_t$ must be determined from the initial conditions of the problem.

2.2 Forced Vibration Solution

The equation of motion governing the forced vibration problem is (1.3.1). On writing this equation in component form,

$$
\begin{aligned}
c_t^2\nabla^2 u_1 + (c_\ell^2 - c_t^2)\frac{\partial}{\partial x_1}(\frac{\partial u_1}{\partial x_1}+\frac{\partial u_2}{\partial x_2}+\frac{\partial u_3}{\partial x_3}) + f_1 &= \frac{\partial^2 u_1}{\partial t^2} \\
c_t^2\nabla^2 u_2 + (c_\ell^2 - c_t^2)\frac{\partial}{\partial x_2}(\frac{\partial u_1}{\partial x_1}+\frac{\partial u_2}{\partial x_2}+\frac{\partial u_3}{\partial x_3}) + f_2 &= \frac{\partial^2 u_2}{\partial t^2} \\
c_t^2\nabla^2 u_3 + (c_\ell^2 - c_t^2)\frac{\partial}{\partial x_3}(\frac{\partial u_1}{\partial x_1}+\frac{\partial u_2}{\partial x_2}+\frac{\partial u_3}{\partial x_3}) + f_3 &= \frac{\partial^2 u_3}{\partial t^2} \ ,
\end{aligned}
\tag{2.2.1}
$$

it can be seen that the three equations are elastically coupled (u_1, u_2, and u_3 appear in each equation). This prevents a straightforward solution, in that the equations must first be uncoupled, an algebraically cumbersome project, even with the use of Laplace transforms. These difficulties can be minimized by expressing the displacement vector in terms of a vector displacement function $\bar{\Psi}$ [14,17,18]:

$$\bar{u} = \rho[c_\ell^2 \nabla^2 \bar{\Psi} - (c_\ell^2 - c_t^2)\nabla\nabla\cdot\bar{\Psi} - \frac{\partial^2 \bar{\Psi}}{\partial t^2}] \ , \qquad (2.2.2)$$

with $\bar{\Psi} = \Psi_1 \hat{e}_1 + \Psi_2 \hat{e}_2 + \Psi_3 \hat{e}_3$

$\Psi_i = \Psi_i(x_1, x_2, x_3, t) \qquad i=1,2,3$

Substituting equation (2.2.2) into equation (2.2.1), one obtains the result

$$(c_\ell^2 \nabla^2 - \frac{\partial^2}{\partial t^2})(c_t^2 \nabla^2 - \frac{\partial^2}{\partial t^2})\bar{\Psi} = -\frac{\bar{f}}{\rho} \ , \qquad (2.2.3)$$

which is the uncoupled equation of motion in terms of the displacement functions. Solving for the $\Psi_i (i=1,2,3)$ from equation (2.2.3) then allows the determination of the displacements from equation (2.2.2).

The solution begins by assuming displacement functions having the same spatial form as the previously assumed normal modes (2.1.3) but now being a general function of time (instead of being restricted to simple harmonic motion):

$$\begin{aligned} \Psi_1 &= \sum_N \sin k_1 x_1 \cos k_2 x_2 \cos k_3 x_3 T_{1N}(t) \\ \Psi_2 &= \sum_N \cos k_1 x_1 \sin k_2 x_2 \cos k_3 x_3 T_{2N}(t) \qquad (2.2.4) \\ \Psi_3 &= \sum_N \cos k_1 x_1 \cos k_2 x_2 \sin k_3 x_3 T_{3N}(t) \ . \end{aligned}$$

These expressions satisfy the boundary conditions, equations (2.1.2). Substituting equation (2.2.4a) into the appropriate uncoupled equation of motion (2.2.3a) and performing the necessary algebraic manipulations, one gets the following results:

$$c_\ell^2 c_t^2 \sum_N \alpha_N^4 \sin k_1 x_1 \cos k_2 x_2 \cos k_3 x_3 T_{1N} + (c_\ell^2 + c_t^2) \sum_N \alpha_N^2 \sin k_1 x_1 \cos k_2 x_2 \cos k_3 x_3 \ddot{T}_{1N} + \sum_N \sin k_1 x_1 \cos k_2 x_2 \cos k_3 x_3 \ddot{\ddot{T}}_{1N} = -\frac{f_1}{\rho} \ , \qquad (2.2.5)$$

where $\ddot{T}_{1N}$ represents the second derivative of $T_{1N}(t)$ with respect to time, etc. The next step is to multiply both sides of equation (2.2.5) by $\sin\ell_1 x_1 \cos\ell_2 x_2 \cos\ell_3 x_3$ and integrate over the spatial domain. However, due to the orthogonality of the normal modes, the following is true:

$$\int_0^{L_1}\int_0^{L_2}\int_0^{L_3} \sin k_1 x_1 \sin\ell_1 x_1 \cos k_2 x_2 \cos\ell_2 x_2 \cos k_3 x_3 \cos\ell_3 x_3 \, dx_1 dx_2 dx_3$$

$$i=1,2,3, \qquad = \begin{cases} 0 & \text{when } \ell_i \neq k_i \\ \dfrac{\eta_1 V}{8} & \text{when } \ell_i = k_i \end{cases}$$

with $\eta_1=(1+\delta_{k_20})(1+\delta_{k_30})$ and $V=L_1L_2L_3$ is the volume of the parallelepiped. Therefore, performing the integrations on equation (2.2.5) gives

$$\ddot{\ddot{T}}_{1N} + (c_\ell^2 + c_t^2)\alpha_N^2 \ddot{T}_{1N} + c_\ell^2 c_t^2 \alpha_N^4 T_{1N} = -\frac{8}{\rho\eta_1 V}\int_0^{L_1}\int_0^{L_2}\int_0^{L_3} f_1 \sin k_1 x_1 \cos k_2 x_2 \cos k_3 x_3 \, dx_1 dx_2 dx_3 . \tag{2.2.6}$$

This expression may be solved by using Laplace transforms and assuming that the motion starts from rest ($T_{1N}(0)=\dot{T}_{1N}(0)=\ddot{T}_{1N}(0)=\ddot{\ddot{T}}_{1N}(0)=0$). Thus,

$$\bar{T}_{1N}(s) = \bar{F}_{1N}(s)\bar{G}_{1N}(s) , \tag{2.2.7}$$

where $\bar{F}_{1N}(s)$ is the transform of the forcing function on the right-hand side of equation (2.2.6) and

$$\bar{G}_{1N}(s) = \frac{1}{(s^2+c_\ell^2\alpha_N^2)(s^2+c_t^2\alpha_N^2)} .$$

Using the convolution property and the fact that $\omega_{\ell N}=c_\ell\alpha_N$ and $\omega_{tN}=c_t\alpha_N$, one can write the inverse transform of equation (2.2.7) as

$$T_{1N}(t) = \int_0^t F_{1N}(\tau)G_{1N}(t-\tau)\,d\tau , \tag{2.2.8}$$

with

$$F_{1N}(\tau) = -\frac{8}{\rho\eta_1 V}\int_0^{L_1}\int_0^{L_2}\int_0^{L_3} f_1(x_1,x_2,x_3,\tau)\sin k_1x_1\cos_2x_2\cos k_3x_3dx_1dx_2dx_3 \tag{2.2.9}$$

$$G_{1M}(t-\tau) = \frac{1}{\omega_{tN}^2-\omega_{\ell N}^2}\left[\frac{\sin\omega_{\ell N}(t-\tau)}{\omega_{\ell N}} - \frac{\sin\omega_{tN}(t-\tau)}{\omega_{tN}}\right]. \tag{2.2.10}$$

The other two uncoupled equations of motion, (2.2.3b) and (2.2.3c), may be treated in a similar fashion with the results

$$T_{2N}(t) = \int_0^t F_{2N}(\tau)G_{2N}(t-\tau)d\tau \tag{2.2.11}$$

$$T_{3N}(t) = \int_0^t F_{3N}(\tau)G_{3N}(t-\tau)d\tau \tag{2.2.12}$$

and

$$F_{2N}(\tau) = -\frac{8}{\rho\eta_2 V}\int_0^{L_1}\int_0^{L_2}\int_0^{L_3} f_2(x_1,x_2,x_3,\tau)\cos k_1x_1\sin k_2x_2\cos k_3x_3dx_1dx_2dx_3 \tag{2.2.13}$$

$$F_{3N}(\tau) = -\frac{8}{\rho\eta_3 V}\int_0^{L_1}\int_0^{L_2}\int_0^{L_3} f_3(x_1,x_2,x_3,\tau)\cos k_1x_1\cos k_2x_2\sin k_3x_3dx_1dx_2dx_3 \tag{2.2.14}$$

$$G_{2N}(t-\tau) = G_{3N}(t-\tau) = \frac{1}{\omega_{tN}^2-\omega_{\ell N}^2}\left[\frac{\sin\omega_{\ell N}(t-\tau)}{\omega_{\ell N}} - \frac{\sin\omega_{tN}(t-\tau)}{\omega_{tN}}\right], \tag{2.2.15}$$

where

$$\eta_2 = (1+\delta_{k_10})(1+\delta_{k_30})$$

$$\eta_3 = (1+\delta_{k_10})(1+\delta_{k_20}) .$$

Finally, equations (2.2.8) through (2.2.15) are substituted into the displacement functions (2.2.4). These in turn are substituted into equation (2.2.2) to arrive at the forced vibration dispalcement $\bar{u}(x_1,x_2,x_3,t)$ for

any generalized body force (per unit mass) $\bar{f}(x_1,x_2,x_3,t)$.

2.3 Response to an Impulse

According to Stephens and Pollock [19], acoutic emission source waves are pulselike functions of stress (force) which are produced by the step displacements associated with material yielding. This model is physically consistent with both plastic deformation and crack propagation, the two major sources of acoustic emission. Assuming a very short duration source event within the body, the Dirac delta function provides an extremely simple mathematical approximation of the resulting impulsive body force. In general, this body force will be three-dimensional; however, here for simplicity it is assumed to be one-dimensional in the x_3 direction and of amplitude F_o. This may be expressed mathematically as

$$\bar{f} = f_3\hat{e}_3$$

$$f_1 = f_2 = 0 \qquad f_3 = F_o\delta(x_1-\xi_1)\delta(x_2-\xi_2)\delta(x_3-\xi_3)\delta(t). \tag{2.3.1}$$

Note that this is an impulsive load applied at the point (ξ_1,ξ_2,ξ_3) and at time $t=0$ (Fig. 2.1).

Substitution of the above impulse into the results of the previous sections gives, from equation (2.2.14),

$$F_3(\tau) = -\frac{8F_o}{\rho\eta_3 V}\cos k_1\xi_1\cos k_2\xi_2\sin k_3\xi_3 . \tag{2.3.2}$$

This result is then combined with equation (2.2.15) and substituted into equation (2.2.12) to produce the time varying portion of the assumed displacement function:

$$T_3(t) = \frac{8F_o\cos k_1\xi_1\cos k_2\xi_2\sin k_3\xi_3}{\rho\eta_3 V(\omega_{\ell N}^2-\omega_{tN}^2)}\left[\frac{\sin\omega_{\ell N}t}{\omega_{\ell N}}-\frac{\sin\omega_{tN}t}{\omega_{tN}}\right] . \tag{2.3.3}$$

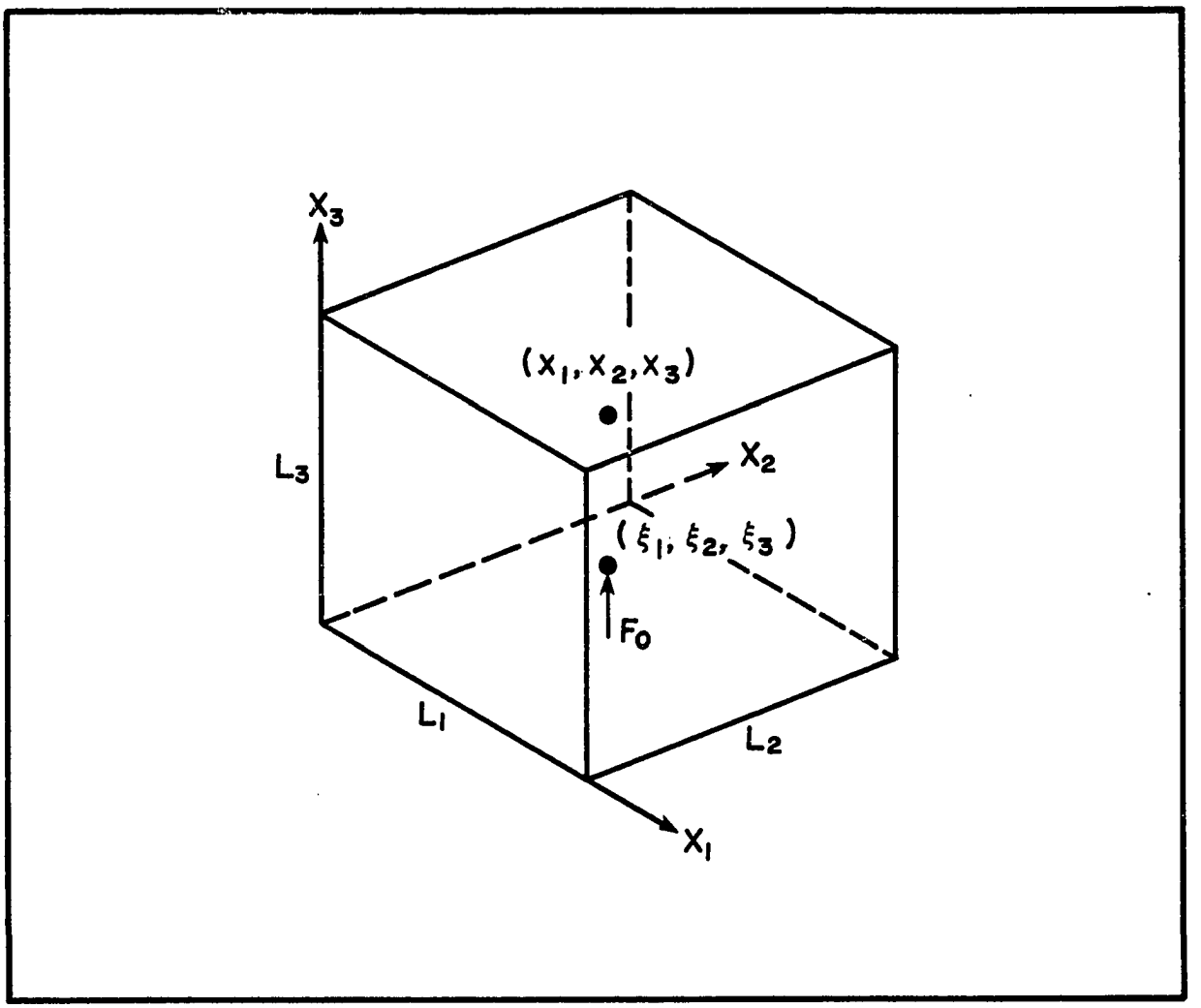

FIGURE 2.1

IMPULSIVE BODY FORCE APPLIED AT THE POINT (ξ_1,ξ_2,ξ_3) AND SENSED AT (x_1,x_2,x_3)

Then from equation (2.2.4) the displacement function becomes

$$\Psi_3 = \sum_N \frac{8F_o \cos k_1\xi_1 \cos k_2\xi_2 \sin k_3\xi_3}{\rho\eta_3 V(\omega_{\ell N}^2 - \omega_{tN}^2)} \cos k_1x_1 \cos k_2x_2 \sin k_3x_3 \left[\frac{\sin\omega_{\ell N}t}{\omega_{\ell N}} - \frac{\sin\omega_{tN}t}{\omega_{tN}}\right]. \tag{2.3.4}$$

Finally, substituting the above into equation (2.2.2) gives the three forced vibration displacement components shown below:

$$\begin{aligned} u_1 &= \sum_N F_o\Phi_{3N} \sin k_1x_1 \cos k_2x_2 \cos k_3x_3 \left[\frac{k_1k_3}{\alpha_N^2}(\Omega_\ell - \Omega_t)\right] \\ u_2 &= \sum_N F_o\Phi_{3N} \cos k_1x_1 \sin k_2x_2 \cos k_3x_3 \left[\frac{k_2k_3}{\alpha_N^2}(\Omega_\ell - \Omega_t)\right] \\ u_3 &= \sum_N F_o\Phi_{3N} \cos k_1x_1 \cos k_2x_2 \sin k_3x_3 \left[\Omega_t + \frac{k_3^2}{\alpha_N^2}(\Omega_\ell - \Omega_t)\right] \ ; \end{aligned} \tag{2.3.5}$$

here

$$\Omega_\ell = \frac{\sin\omega_{\ell N}t}{\omega_{\ell N}}$$

$$\Omega_t = \frac{\sin\omega_{tN}t}{\omega_{tN}}$$

and

$$\Phi_{3N} = \frac{8}{\eta_3 V} \cos k_1\xi_1 \cos k_2\xi_2 \sin k_3\xi_3 \ .$$

Not surprisingly, these results are the same as those obtained by Hill and Egle [20] using a Green's function approach to the problem.

2.4 Symmetric Boundary Conditions

Algebraically, it is often advantageous to work a problem over a symmetric interval. As such, the free and forced vibration solutions for the rectangular parallelepiped with completely rigid-lubricated

faces are presented here for the symmetric boundary conditions

$$\begin{aligned} x_1 &= -\frac{L_1}{2}, \frac{L_1}{2} & u_1 &= 0 & \frac{\partial u_2}{\partial x_1} &= \frac{\partial u_3}{\partial x_1} = 0 \\ x_2 &= -\frac{L_2}{2}, \frac{L_2}{2} & u_2 &= 0 & \frac{\partial u_1}{\partial x_2} &= \frac{\partial u_3}{\partial x_2} = 0 \\ x_3 &= -\frac{L_3}{2}, \frac{L_3}{2} & u_3 &= 0 & \frac{\partial u_1}{\partial x_3} &= \frac{\partial u_2}{\partial x_3} = 0 \end{aligned} \qquad (2.4.1)$$

For the free vibration solution, the equation of motion is again equation (2.1.1). Assuming normal modes of the form

$$\begin{aligned} u_{1N} &= A_{1N}\sin k_1(x_1+\tfrac{L_1}{2})\cos k_2(x_2+\tfrac{L_2}{2})\cos k_3(x_3+\tfrac{L_3}{2})\sin\omega_N t \\ u_{2N} &= A_{2N}\cos k_1(x_1+\tfrac{L_1}{2})\sin k_2(x_2+\tfrac{L_2}{2})\cos k_3(x_3+\tfrac{L_3}{2})\sin\omega_N t \\ u_{3N} &= A_{3N}\cos k_1(x_1+\tfrac{L_1}{2})\cos k_2(x_2+\tfrac{L_2}{2})\sin k_3(x_3+\tfrac{L_3}{2})\sin\omega_N t \end{aligned} \qquad (2.4.2)$$

and proceeding as in Section 2.1, identical results are obtained for the wave numbers, characteristic equation, natural frequencies and the amplitude relations. Therefore, the free vibration displacements for the symmetric boundary conditions may be written as

$$u_1 = \sum_N \sin k_1(x_1+\tfrac{L_1}{2})\cos k_2(x_2+\tfrac{L_2}{2})\cos k_3(x_3+\tfrac{L_3}{2})\{(A_{1N})_\ell \sin\omega_{\ell N} t + (A_{1N})_t \sin\omega_{tN} t\}$$

$$u_2 = \sum_N \cos k_1(x_1+\tfrac{L_1}{2})\sin k_2(x_2+\tfrac{L_2}{2})\cos k_3(x_3+\tfrac{L_3}{2})\{\tfrac{k_2}{k_1}(A_{1N})_\ell \sin\omega_{\ell N} t + (A_{2N})_t \sin\omega_{tN} t\} \qquad (2.4.3)$$

$$u_3 = \sum_N \cos k_1(x_1+\tfrac{L_1}{2})\cos k_2(x_2+\tfrac{L_2}{2})\sin k_3(x_3+\tfrac{L_3}{2})\{\tfrac{k_3}{k_1}(A_{1N})_\ell \sin\omega_{\ell N} t - [\tfrac{k_1}{k_3}(A_{1N})_t + \tfrac{k_2}{k_3}(A_{2N})_t]\sin\omega_{tN} t\} .$$

The forced vibration solution may be handled similarly. Assuming that the displacement functions can be expressed as

$$\Psi_1 = \sum_N \sin k_1(x_1+\tfrac{L_1}{2})\cos k_2(x_2+\tfrac{L_2}{2})\cos k_3(x_3+\tfrac{L_3}{2})T_{1N}(t)$$

$$\Psi_2 = \sum_N \cos k_1(x_1+\tfrac{L_1}{2})\sin k_2(x_2+\tfrac{L_2}{2})\cos k_3(x_3+\tfrac{L_3}{2})T_{2N}(t) \qquad (2.4.4)$$

$$\Psi_3 = \sum_N \cos k_1(x_1+\tfrac{L_1}{2})\cos k_2(x_2+\tfrac{L_2}{2})\sin k_3(x_3+\tfrac{L_3}{2})T_{3N}(t)$$

and following the same procedure as in Section 2.2, one obtains similar results, the only difference being in the arguments of the spatial sin and cos terms. Instead of k_1x_1, k_2x_2, and k_3x_3, these arguments should be $k_1(x_1+\frac{L_1}{2})$, $k_2(x_2+\frac{L_2}{2})$ and $k_3(x_3+\frac{L_3}{2})$. In all other respects the functions are identical.

CHAPTER III

STRESS-FREE/RIGID-LUBRICATED BOUNDARIES

3.1 Free Vibration Solution

The applicable equation of motion for the free vibration solution is (2.1.1), which is repeated here for convenience:

$$c_t^2\nabla^2\bar{u} + (c_\ell^2 - c_t^2)\nabla\nabla\cdot\bar{u} = \frac{\partial^2\bar{u}}{\partial t^2} \ . \tag{3.1.1}$$

The boundary conditions consist of two stress-free faces and four rigid-lubricated faces and can be written as

$$\begin{array}{lll} x_1 = 0,L_1 & u_1 = 0 & \dfrac{\partial u_2}{\partial x_1} = \dfrac{\partial u_3}{\partial x_1} = 0 \\ x_2 = 0,L_2 & u_2 = 0 & \dfrac{\partial u_1}{\partial x_2} = \dfrac{\partial u_3}{\partial x_2} = 0 \\ x_3 = 0,L_3 & \dfrac{\partial u_1}{\partial x_1} + \dfrac{\partial u_2}{\partial x_2} + \gamma\dfrac{\partial u_3}{\partial x_3} = 0 & \dfrac{\partial u_3}{\partial x_1} + \dfrac{\partial u_1}{\partial x_3} = \dfrac{\partial u_3}{\partial x_2} + \dfrac{\partial u_2}{\partial x_3} = 0 \end{array} \tag{3.1.2}$$

A pictorial presentation of this system is shown in Figure 3.1. The specimen has a finite elastic modulus and is enclosed on four sides by an infinitely rigid medium such that normal displacements at these four surfaces are zero. However, due to lubrication between the contacting surfaces, transverse motion is uninhibited. The two x_3 faces (cross-hatched) are stress-free and, as a result, incident waves will mode convert on reflection. The two x_1 faces and the two x_2 faces, being rigid-lubricated, will reflect with no mode conversion. Thus, as

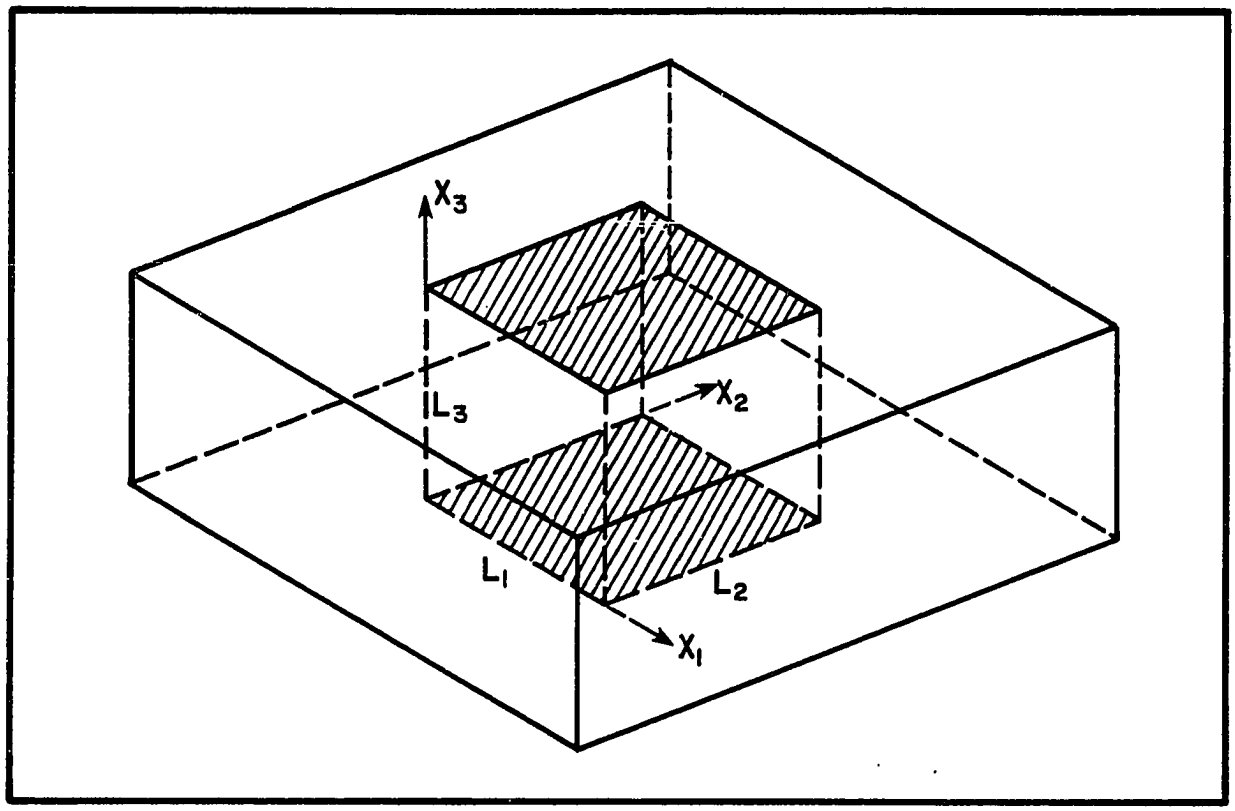

FIGURE 3.1
STRESS-FREE/RIGID-LUBRICATED BOUNDARIES

the boundary conditions become more complex, so also does the wave propagation. This increase in complexity holds true for the normal modes and the characteristic equation as well. Where in Chapter II it was possible to determine by inspection the exact form of the normal modes, this no longer holds true; rather, considerable calculation is required.

These calculations begin with the Helmholtz resolution [11, 21], which says that any vector field may be resolved into the gradient of a scalar and the curl of a zero-divergence vector. The vector field of interest here is displacement; hence,

$$\bar{u} = \nabla S + \nabla \times \bar{V} \tag{3.1.3}$$

$$\nabla \cdot \bar{V} = 0 \ , \tag{3.1.4}$$

where

$S = S(x_1,x_2,x_3,t)$ = scalar potential

$\bar{V} = V_1\hat{e}_1 + V_2\hat{e}_2 + V_3\hat{e}_3$ = vector potential

and $V_i = V_i(x_1,x_2,x_3,t)$, $i=1,2,3$. Substitution of equation (3.1.3) into the equation of motion (3.1.1) leads to the separated wave equations (c.f. Appendix A):

$$\nabla^2 S = \frac{1}{c_\ell^{\,2}} \frac{\partial^2 S}{\partial t^2} \tag{3.1.5}$$

$$\nabla^2 \bar{V} = \frac{1}{c_t^{\,2}} \frac{\partial^2 \bar{V}}{\partial t^2} \ . \tag{3.1.6}$$

From the above equations it can be seen that the scalar potential is associated with dilatational (or infinite sums of component plane longitudinal) waves and the vector potential with equivoluminal (transverse) waves. As such, equation (3.1.3) may then be rewritten as

$$\bar{u} = \bar{u}^D + \bar{u}^E \tag{3.1.7}$$

with

$$\bar{u}^D = \nabla S = \frac{\partial S}{\partial x_1}\hat{e}_1 + \frac{\partial S}{\partial x_2}\hat{e}_2 + \frac{\partial S}{\partial x_3}\hat{e}_3 = u_1^D\hat{e} + u_2^D\hat{e} + u_3^D\hat{e} \tag{3.1.8}$$

$$\bar{u}^E = \nabla \times \bar{V} = \left(\frac{\partial V_3}{\partial x_2} - \frac{\partial V_2}{\partial x_3}\right)\hat{e}_1 + \left(\frac{\partial V_1}{\partial x_3} - \frac{\partial V_3}{\partial x_1}\right)\hat{e}_2 + \left(\frac{\partial V_2}{\partial x_1} - \frac{\partial V_1}{\partial x_2}\right)\hat{e}_3 = u_1^E\hat{e}_1 + u_2^E\hat{e}_2 + u_3^E\hat{e}_3. \tag{3.1.9}$$

The superscripts D and E denote the dilatational and equivoluminal components respectively. Thus, the Helmholtz resolution mathematically uncouples the wave motion such that the dilatational and equivoluminal components can be dealt with separately. The price for this convenience is one additional equation, the zero divergence gauge condition (3.1.4). In other words, there are now four equations to solve, instead of three, for the three displacement components (u_1, u_2, u_3).

The general solutions of the separated wave equations, (3.1.5) and (3.1.6), as developed in Appendix A, may be particularized to fit the boundary conditions (3.1.2) and the Helmholtz resolution (3.1.3). Hence, the scalar and vector potentials must be of the form

$$S_N = -\cos k_1 x_1 \cos k_2 x_2 (A_{1N}\cos k_\ell x_3 + A_{2N}\sin k_\ell x_3)\sin\omega_N t \tag{3.1.10}$$

and

$$\begin{aligned} V_{1N} &= \cos k_1 x_1 \sin k_2 x_2 (B_{1N}\cos k_t x_3 + B_{2N}\sin k_t x_3)\sin\omega_N t \\ V_{2N} &= \sin k_1 x_1 \cos k_2 x_2 (C_{1N}\cos k_t x_3 + C_{2N}\sin k_t x_3)\sin\omega_N t \\ V_{3N} &= \sin k_1 x_1 \sin k_2 x_2 (D_{1N}\cos k_t x_3 + D_{2N}\sin k_t x_3)\sin\omega_N t \ . \end{aligned} \tag{3.1.11}$$

These are corrections to those presented by Kaliski [12]. The associated

wave numbers are given as

$$k_\ell = \left[\frac{\omega_N^2}{c_\ell^2} - (k_1^2 + k_2^2)\right]^{\frac{1}{2}} \tag{3.1.12}$$

$$k_t = \left[\frac{\omega_N^2}{c_t^2} - (k_1^2 + k_2^2)\right]^{\frac{1}{2}} , \tag{3.1.13}$$

where $k_1 = \frac{n_1\Pi}{L_1}$ and $k_2 = \frac{n_2\Pi}{L_2}$ as before (n_i=0,1,2,...; i=1,2). On substituting the assumed potentials, equations (3.1.10) and (3.1.11), into equations (3.1.8) and (3.1.9), one finds the normal modes of the dilatational and equivoluminal displacement components to be

$$\begin{aligned}
u_{1N}^D &= \sin k_1 x_1 \cos k_2 x_2 [k_1 (A_{1N} \cos k_\ell x_3 + A_{2N} \sin k_\ell x_3)] \sin\omega_N t = \phi_{1N}^D \sin\omega_N t \\
u_{2N}^D &= \cos k_1 x_1 \sin k_2 x_2 [k_2 (A_{1N} \cos k_\ell x_3 + A_{2N} \sin k_\ell x_3)] \sin\omega_N t = \phi_{2N}^D \sin\omega_N t \\
u_{3N}^D &= \cos k_1 x_1 \cos k_2 x_2 [k_\ell (A_{1N} \sin k_\ell x_3 - A_{2N} \cos k_\ell x_3)] \sin\omega_N t = \phi_{3N}^D \sin\omega_N t
\end{aligned} \tag{3.1.14}$$

$$\begin{aligned}
u_{1N}^E &= \sin k_1 x_1 \cos k_2 x_2 [(k_2 D_{1N} - k_t C_{2N}) \cos k_t x_3 + (k_2 D_{2N} + k_t C_{1N}) \sin k_t x_3] \sin\omega_N t \\
u_{2N}^E &= \cos k_1 x_1 \sin k_2 x_2 [(k_t B_{2N} - k_1 D_{1N}) \cos k_t x_3 - (k_1 D_{2N} + k_t B_{1N}) \sin k_t x_3] \sin\omega_N t \\
u_{3N}^E &= \cos k_1 x_1 \cos k_2 x_2 [(k_1 C_{1N} - k_2 B_{1N}) \cos k_t x_3 + (k_1 C_{2N} - k_2 B_{2N}) \sin k_t x_3] \sin\omega_N t .
\end{aligned} \tag{3.1.15}$$

Application of the zero divergence gauge condition (3.1.4) to the vector potential $\bar{V}$ leads to the result that

$$D_{1N} = -\frac{1}{k_t}(k_1 B_{2N} + k_2 C_{2N})$$

$$D_{2N} = \frac{1}{k_t}(k_1 B_{1N} + k_2 C_{1N}) ,$$

which allows a simplification of equation (3.1.15) to

$$u^E_{1N} = \sin k_1x_1\cos k_2x_2\{-\frac{1}{k_t}[k_1k_2B_{2N} + (k_2^2+k_t^2)C_{2N}]\cos k_tx_3$$
$$+ \frac{1}{k_t}[k_1k_2B_{1N} + (k_2^2+k_t^2)C_{1N}]\sin k_tx_3\}\sin\omega_Nt$$

$$u^E_{2N} = \cos k_1x_1\sin k_2x_2\{\frac{1}{k_t}[(k_1^2+k_t^2)B_{2N} + k_1k_2C_{2N}]\cos k_tx_3 \qquad (3.1.16)$$
$$- \frac{1}{k_t}[(k_1^2+k_t^2)B_{1N} + k_1k_2C_{1N}]\sin k_tx_3\}\sin\omega_Nt$$

$$u^E_{3N} = \cos k_1x_1\cos k_2x_2\{(k_1C_{1N} - k_2B_{1N})\cos k_tx_3 + (k_1C_{2N} - k_2B_{2N})\sin k_tx_3\}\sin\omega_Nt.$$

The equivoluminal displacement components may be put into the same form as Kaliski's [12] by letting

$$A_{3N} = -\frac{1}{k_t}[k_1k_2B_{2N} + (k_2^2+k_t^2)C_{2N}]$$

$$A_{4N} = \frac{1}{k_t}[k_1k_2B_{1N} + (k_2^2+k_t^2)C_{1N}]$$

$$A_{5N} = \frac{1}{k_t}[(k_1^2+k_t^2)B_{2N} + k_1k_2C_{2N}]$$

$$A_{6N} = -\frac{1}{k_t}[(k_1^2+k_t^2)B_{1N} + k_1k_2C_{1N}],$$

and substituting these amplitudes into equation (3.1.16). This yields the results

$$u^E_{1N} = \sin k_1x_1\cos k_2x_2(A_{3N}\cos k_tx_3 + A_{4N}\sin k_tx_3)\sin\omega_Nt = \Phi^E_{1N}\sin\omega_Nt$$

$$u^E_{2N} = \cos k_1x_1\sin k_2x_2(A_{5N}\cos k_tx_3 + A_{6N}\sin k_tx_3)\sin\omega_Nt = \Phi^E_{2N}\sin\omega_Nt$$

$$u_{3N}^{E} = \cos k_1 x_1 \cos k_2 x_2 \{\frac{1}{k_t}[(k_1 A_{4N} + k_2 A_{6N})\cos k_t x_3 - (k_1 A_{3N} + k_2 A_{5N})\sin k_t x_3]\}\sin\omega_N t = \phi_{2N}^{E}\sin\omega_N t. \tag{3.1.17}$$

The dilatational and equivoluminal displacements, equations (3.1.14) and (3.1.17) may then be combined according to equation (3.1.7) to generate the normal mode displacement components obtained by Kaliski [12]:

$$\begin{aligned} u_{1N} &= (\phi_{1N}^{D} + \phi_{1N}^{E})\sin\omega_N t = \phi_{1N}\sin\omega_N t \\ u_{2N} &= (\phi_{2N}^{D} + \phi_{2N}^{E})\sin\omega_N t = \phi_{2N}\sin\omega_N t \\ u_{3N} &= (\phi_{3N}^{D} + \phi_{3N}^{E})\sin\omega_N t = \phi_{3N}\sin\omega_N t. \end{aligned} \tag{3.1.18}$$

The next step is to determine the natural frequencies of the system. This is accomplished by substituting the above normal modes into the boundary conditions (3.1.2). Twelve of the eighteen boundary conditions are satisfied exactly, leaving six equations in the six unknowns $A_{iN}(i=1,2,\ldots,6)$:

$$\begin{aligned} &(k_1^2 + k_2^2 + \gamma k_\ell^2)A_{1N} - (\gamma-1)k_1 A_{3N} - (\gamma-1)k_2 A_{5N} = 0 \\ &(k_1^2 + k_2^2 + \gamma k_\ell^2)\cos k_\ell L_3 A_{1N} + (k_1^2 + k_2^2 + \gamma k_\ell^2)\sin k_\ell L_3 A_{2N} - (\gamma-1)k_1\cos k_t L_3 A_{3N} \\ &\quad - (\gamma-1)k_1\sin k_t L_3 A_{4N} - (\gamma-1)k_2\cos k_t L_3 A_{5N} - (\gamma-1)k_2\sin k_t L_3 A_{6N} = 0 \\ &2k_1 k_\ell k_t A_{2N} - (k_1^2 - k_t^2)A_{4N} - k_1 k_2 A_{6N} = 0 \end{aligned} \tag{3.1.19}$$

$$- 2k_1k_\ell k_t \sin k_\ell L_3 A_{1N} + 2k_1k_\ell k_t \cos k_\ell L_3 A_{2N} + (k_1^2 - k_t^2)\sin k_t L_3 A_{3N}$$
$$- (k_1^2 - k_t^2)\cos k_t L_3 A_{4N} + k_1k_2 \sin k_t L_3 A_{5N} - k_1k_2 \cos k_t L_3 A_{6N} = 0$$

$$2k_2k_\ell k_t A_{2N} - k_1k_2 A_{4N} - (k_2^2 - k_t^2)A_{6N} = 0$$

$$- 2k_2k_\ell k_t \sin k_\ell L_3 A_{1N} + 2k_2k_\ell k_t \cos k_\ell L_3 A_{2N} + k_1k_2 \sin k_t L_3 A_{3N}$$
$$- k_1k_2 \cos k_t L_3 A_{4N} + (k_2^2 - k_t^2)\sin k_t L_3 A_{5N} - (k_2^2 - k_t^2)\cos k_t L_3 A_{6N} = 0 \ .$$

The amplitude relations and frequency equations are determined from these six expressions. There are several appropriate combinations depending upon the values of $\sin k_t L_3$ and the wave numbers k_1 and k_2. These are summarized in Table 3.1.

The first combination includes amplitude relations (3.1.20) and the frequency equation (3.1.21); this applies when $\sin k_t L_3 = 0$ and $k_1 > 0$, $k_2 > 0$. It represents horizontally polarized (displacements in $x_1 - x_2$ plane only) shear waves and is sometimes referred to as an SH wave solution. From equations (3.1.14), (3.1.17), and (3.1.18), it can be seen that this solution contributes nothing to the u_3 displacement component and allows for no mode conversions at the boundaries.

The amplitude relations and frequency equation associated with $\sin k_t L_3 \neq 0$ and $k_1 = k_2 = 0$ are (3.1.22) and (3.1.23), respectively. The latter is derived from the fact that the only meaningful solution to equations (3.1.19) comes when $\sin k_\ell L_3 = 0$ and $A_{2N} \neq 0$. These are longitudinal waves propagating in the x_3 direction, and because they are normally incident on the stress-free surfaces, there are no mode conversions. They simply reflect back and forth between the two faces.

TABLE 3.1. Appropriate Modal Coefficients and Frequency Equations, Stress-Free/Rigid-Lubricated Boundaries

Modal Coefficients	$\sin k_t L_3 = 0$	$\sin k_t L_3 \neq 0$		
	$k_1 > 0,\ k_2 > 0$	$k_1 = k_2 = 0$	$k_1 > 0,\ k_2 = 0$	$k_1 \geq 0,\ k_2 = 0$
A_{1N}	0	0	$-\frac{P}{R}\left(\frac{k_1^2-k_t^2}{2k_1k_\ell k_t}\right)A_{3N}$	$-\frac{P}{R}\left(\frac{k_1^2+k_2^2-k_t^2}{2k_2k_\ell k_t}\right)A_{5N}$
A_{2N}	0	*	$\frac{k_1^2-k_t^2}{2k_1k_\ell k_t}A_{4N}$	$\frac{k_1^2+k_2^2-k_t^2}{2k_2k_\ell k_t}A_{6N}$
A_{3N}	$-\frac{k_2}{k_1}A_{5N}$	0	$-\frac{R(\cos k_\ell L_3-\cos k_t L_3)}{P\sin k_\ell L_3+R\sin k_t L_3}A_{4N}$	$\frac{k_1}{k_2}A_{5N}$
A_{4N}	0	0	*	$\frac{k_1}{k_2}A_{6N}$
A_{5N}	*	0	0	$-\frac{R(\cos k_\ell L_3-\cos k_t L_3)}{P\sin k_\ell L_3+R\sin k_t L_3}A_{6N}$
A_{6N}	0	0	0	*
	(3.1.20)	(3.1.22)	(3.1.24)	(3.1.25)
Frequency Equations	$\omega_N = c_t\alpha$ (3.1.21)	$\omega_N = c_\ell\alpha$ (3.1.23)	$(P^2+R^2)\sin k_\ell L_3 \sin k_t L_3 + 2PR(1-\cos k_\ell L_3 \cos k_t L_3) = 0$ (3.1.26)	
	$\alpha^2 = k_1^2+k_2^2+k_3^2$		$P = 4(k_1^2+k_2^2)k_\ell k_t$ $\quad R = (k_1^2+k_2^2-k_t^2)^2$	

* For the free vibration problem, these values are determined from the initial conditions; in the forced vibration problem, from the forcing function.

The last two sets of amplitude relations, (3.1.24) and (3.1.25), share the frequency equation (3.1.26). This equation is obtained by setting the determinant of equations (3.1.19) equal to zero and dividing the result by $\sin k_t L_3$, since $\sin k_t L_3 \neq 0$. Whereas for the completely rigid-lubricated problem the natural frequencies of each of the plane wave components $N(n_1,n_2,n_3)$ could be determined explicitly from the frequency equation (2.1.5), here they must be solved for implicitly because (3.1.26) is a transcendental equation, which allows for mode conversions at the two stress-free surfaces. These mode conversions are responsible for the increased complexity in the amplitude relations. Equations (3.1.24), (3.1.25), and (3.1.26) thus describe the motion of the mode converting longitudinal and vertically polarized shear waves. This solution is also referred to as the SV/P wave solution.

Notice that the case $\sin k_t L_3 \neq 0$ and $k_1 > 0$, $k_2 = 0$ corresponds to modes in which the shear waves propagate in $x_1 - x_3$ planes only. Consequently, there are no equivoluminal displacements in the x_2 direction, i.e., $u^E_{2N} = 0$ (ref. equation (3.1.17b)). When $\sin k_t L_3 \neq 0$ and $k_1 = 0$, $k_2 > 0$, the inverse condition exists: shear waves propagate in $x_2 - x_3$ planes only, and as a result, $u^E_{1N} = 0$.

For the free vibration problem, the amplitudes designated by the asterisks in Table 3.1 are determined from the initial conditions; in the forced vibration problem of the ensuing section, they are determined from the forcing function. The expressions for P and R and the amplitude relations A_{1N}, A_{2N}, and A_{5N} from (3.1.25) are all corrections to Kaliski's free vibration solution [12], as are the assumed scalar and vector potentials, equations (3.1.10) and (3.1.11).

Each of the normal modes defined by equations (3.1.18) represents a plane wave component traveling in a direction determined by the set $N(n_1,n_2,n_3)$, where n_1 and n_2 specify the wave numbers $k_1 = n_1\pi/L_1$ and $k_2 = n_2\pi/L_2$ and n_3 refers to the infinite set of natural frequencies. The three-dimensional free vibration displacement components are then made up of the infinity of plane wave components N traveling in all directions:

$$u_1(x_1,x_2,x_3) = \sum_N u_{1N}(x_1,x_2,x_3)$$

$$u_2(x_1,x_2,x_3) = \sum_N u_{2N}(x_1,x_2,x_3) \qquad (3.1.27)$$

$$u_3(x_1,x_2,x_3) = \sum_N u_{3N}(x_1,x_2,x_3) \quad ,$$

with $\sum_N = \sum_{n_1=0}^{\infty} \sum_{n_2=0}^{\infty} \sum_{n_3=0}^{\infty}$, as before.

3.2 Forced Vibration Solution

The equation of interest for the forced vibration solution is

$$c_t^2\nabla^2\bar{u} + (c_\ell^2 - c_t^2)\nabla\nabla\cdot\bar{u} + \bar{f} = \frac{\partial^2\bar{u}}{\partial t^2} \quad , \tag{3.2.1}$$

and the displacement vector is assumed to be of the form [22]

$$\bar{u} = \sum_N \bar{\phi}_N(x_1,x_2,x_3)T_N(t) \quad , \tag{3.2.2}$$

where

$$\bar{\phi}_N = \phi_{1N}\hat{e}_1 + \phi_{2N}\hat{e}_2 + \phi_{3N}\hat{e}_3 \quad .$$

and the $\phi_{iN}(i=1,2,3)$ are the modal functions defined by equations (3.1.14), (3.1.17), and (3.1.18). Note that these functions represent the spatial portion of the normal modes, and as such, they satisfy the rigid-lubricated/stress-free boundary conditions, equations (3.1.2).

Substitution of the assumed displacement (3.2.2) into the governing equation of motion (3.2.1) produces the result

$$\sum_N [c_t^2\nabla^2\bar{\phi}_N + (c_\ell^2 - c_t^2)\nabla\nabla\cdot\bar{\phi}_N]T_N + \bar{f} = \sum_N \bar{\phi}_N\ddot{T}_N \quad . \tag{3.2.3}$$

The bracketed term on the left hand side of this expression may be simplified by substituting the free vibration displacements of equations (3.1.23),

$$\bar{u} = \sum_N \bar{\phi}_N \sin\omega_N t \quad , \tag{3.2.4}$$

into the free vibration equation of motion (3.1.1); thus

$$c_t^2\nabla^2\bar{\phi}_N + (c_\ell^2 - c_t^2)\nabla\nabla\cdot\bar{\phi}_N = -\omega_N\bar{\phi}_N \quad . \tag{3.2.5}$$

Equation (3.2.5) is then substituted into equation (3.2.3) and the results rearranged:

$$\sum_N \bar{\phi}_N(\ddot{T}_N + \omega_N^2 T_N) = \bar{f}. \tag{3.2.6}$$

Taking the scalar product of both sides of this equation with $\bar{\phi}_M$, where $M(m_1,m_2)$ denotes another modal function, and integrating over the spatial domain, one gets

$$\sum_N (\ddot{T}_N + \omega_N^2 T_N) \int_V \bar{\phi}_N \cdot \bar{\phi}_M dV = \int_V \bar{f} \cdot \bar{\phi}_M dV \ . \tag{3.2.7}$$

It can be shown that the governing equations are self-adjoint; consequently, the $\bar{\phi}_N$ must be orthogonal [23]. This means that

$$\int_V \bar{\phi}_N \cdot \bar{\phi}_M dV = 0 \quad N(n_1,n_2) \neq M(m_1,m_2), \tag{3.2.8}$$

and therefore,

$$\ddot{T}_N + \omega_N^2 T_N = W_N \tag{3.2.9}$$

with

$$W_N(t) = \frac{1}{E_N} \int_0^{L_1}\int_0^{L_2}\int_0^{L_3} \bar{f}(x_1,x_2,x_3,t) \cdot \bar{\phi}_N(x_1,x_2,x_3) dx_1 dx_2 dx_3 \tag{3.2.10}$$

$$E_N = \int_0^{L_1}\int_0^{L_2}\int_0^{L_3} \bar{\phi}_N \cdot \bar{\phi}_N dx_1 dx_2 dx_2. \tag{3.2.11}$$

The quantity E_N represents the generalized mass per unit density.

The generalized time varying function $T_N(t)$ is found by assuming that the motion starts from rest ($T_N(0)=\dot{T}_N(0)=0$) and taking Laplace transforms:

$$\bar{T}_N(s) = \bar{V}_N(s)\bar{W}_N(s) \ . \tag{3.2.12}$$

Here

$$\bar{V}_N(s) = \frac{1}{s^2 + \omega_N^2} \tag{3.2.13}$$

and $\bar{W}_N(s)$ is the transform of equation (3.2.10). The inverse transforms of equations (3.2.12) and (3.2.13), when combined, yield the desired result

$$T_N(t) = \frac{1}{\omega_N} \int_0^t W_N(\tau) \sin\omega_N(t-\tau) d\tau \ . \tag{3.2.14}$$

The forced vibration displacements are obtained by substituting the above back into equation (3.2.2). Hence, in component form they become

$$\begin{aligned} u_1(x_1,x_2,x_3,t) &= \sum_N \phi_{1N}(x_1,x_2,x_3) T_N(t) \\ u_2(x_1,x_2,x_3,t) &= \sum_N \phi_{2N}(x_1,x_2,x_3) T_N(t) \\ u_3(x_1,x_2,x_3,t) &= \sum_N \phi_{3N}(x_1,x_2,x_3) T_N(t) \ . \end{aligned} \tag{3.2.15}$$

The time varying function T_N may be determined for any generalized body force (per unit mass) according to equations (3.2.10), (3.2.11), and (3.2.14).

3.3 Response to an Impulse

The impulsive body force assumed here is the same as that employed in Chapter II and is written as

$$\bar{f}(x_1,x_2,x_3,t) = F_o \delta(x_1 - \xi_1)\delta(x_2 - \xi_2)\delta(x_3 - \xi_3)\delta(t)\hat{e}_3 \ . \tag{3.3.1}$$

On substituting this expression into equation (3.2.10), one obtains

$$W_N(t) = \frac{F_o}{E_N} \phi_{3N}(\xi_1,\xi_2,\xi_3)\delta(t) \ . \tag{3.3.2}$$

In order to get the time varying function T_N, the above is substituted into equation (3.2.14). Integration then yields

$$T_N(t) = \frac{F_o}{E_N \omega_N} \phi_{3N}(\xi_1,\xi_2,\xi_3)\sin\omega_N t \ . \tag{3.3.3}$$

This is then combined with equation (3.2.15) to obtain the displacement components produced by a one-dimensional impulse of magnitude F_o applied in the x_3 direction at the point (ξ_1,ξ_2,ξ_3):

$$\begin{aligned}
u_1(x_1,x_2,x_3,t) &= \sum_N \frac{F_o}{E_N \omega_N} \phi_{3N}(\xi_1,\xi_2,\xi_3)\phi_{1N}(x_1,x_2,x_3)\sin\omega_N t \\
u_2(x_1,x_2,x_3,t) &= \sum_N \frac{F_o}{E_N \omega_N} \phi_{3N}(\xi_1,\xi_2,\xi_3)\phi_{2N}(x_1,x_2,x_3)\sin\omega_N t \\
u_3(x_1,x_2,x_3,t) &= \sum_N \frac{F_o}{E_N \omega_N} \phi_{3N}(\xi_1,\xi_2,\xi_3)\phi_{3N}(x_1,x_2,x_3)\sin\omega_N t .
\end{aligned} \tag{3.3.4}$$

In performing the calculations, the ω_N are determined from the characteristic equation (3.1.20) and the quantity E_N is evaluated in Appendix B.

3.4 Symmetric Boundary Conditions

The symmetric boundary conditions for the parallelepiped with two stress-free and four rigid-lubricated boundaries are

$$\begin{array}{lll}
x_1 = -\frac{L_1}{2}, \frac{L_1}{2} & u_1 = 0 & \frac{\partial u_2}{\partial x_1} = \frac{\partial u_3}{\partial x_1} = 0 \\
x_2 = -\frac{L_2}{2}, \frac{L_2}{2} & u_2 = 0 & \frac{\partial u_1}{\partial x_2} = \frac{\partial u_3}{\partial x_2} = 0 \\
x_3 = -\frac{L_3}{2}, \frac{L_3}{2} & \frac{\partial u_1}{\partial x_1}+\frac{\partial u_2}{\partial x_2}+\gamma\frac{\partial u_3}{\partial x_3} = 0 & \frac{\partial u_3}{\partial x_1}+\frac{\partial u_1}{\partial x_3} = \frac{\partial u_3}{\partial x_2}+\frac{\partial u_2}{\partial x_3} = 0 \ .
\end{array} \tag{3.4.1}$$

Once again, the equation of motion for the free vibration solution is equation (3.1.1). Here the scalar and vector potentials are assumed

to be

$$S_N = -\cos k_1(x_1+\tfrac{L_1}{2})\cos k_2(x+\tfrac{L_2}{2})[A_{1N}\cos k_\ell(x_3+\tfrac{L_3}{2})+A_{2N}\sin k_\ell(x_3+\tfrac{L_3}{2})]\sin\omega_N t \tag{3.4.2}$$

and

$$\begin{aligned}
V_{1N} &= \cos k_1(x_1+\tfrac{L_1}{2})\sin k_2(x_2+\tfrac{L_2}{2})[B_{1N}\cos k_t(x_3+\tfrac{L_3}{2})+B_{2N}\sin k_t(x_3+\tfrac{L_3}{2})]\sin\omega_N t\\
V_{2N} &= \sin k_1(x_1+\tfrac{L_1}{2})\cos k_2(x_2+\tfrac{L_2}{2})[C_{1N}\cos k_t(x_3+\tfrac{L_3}{2})+C_{2N}\sin k_t(x_3+\tfrac{L_3}{2})]\sin\omega_N t\\
V_{3N} &= \sin k_1(x_1+\tfrac{L_1}{2})\sin k_2(x_2+\tfrac{L_2}{2})[D_{1N}\cos k_t(x_3+\tfrac{L_3}{2})+D_{2N}\sin k_t(x_3+\tfrac{L_3}{2})]\sin\omega_N t
\end{aligned} \tag{3.4.3}$$

Following the same procedure as in Section 3.1 results in the normal mode displacement components

$$\begin{aligned}
u_{1N} &= \sin k_1(x_1+\tfrac{L_1}{2})\cos k_2(x_2+\tfrac{L_2}{2})\{k_1[A_{1N}\cos k_\ell(x_3+\tfrac{L_3}{2})+A_{2N}\sin k_\ell(x_3+\tfrac{L_3}{2})]\\
&\qquad + A_{3N}\cos k_t(x_3+\tfrac{L_3}{2})+A_{4N}\sin k_t(x_3+\tfrac{L_3}{2})\}\sin\omega_N t\\
u_{2N} &= \cos k_1(x_1+\tfrac{L_1}{2})\sin k_2(x_2+\tfrac{L_2}{2})\{k_2[A_{1N}\cos k_\ell(x_3+\tfrac{L_3}{2})+A_{2N}\sin k_\ell(x_3+\tfrac{L_3}{2})]\\
&\qquad + A_{5N}\cos k_t(x_3+\tfrac{L_3}{2})+A_{6N}\sin k_t(x_3+\tfrac{L_3}{2})\}\sin\omega_N t\\
u_{3N} &= \cos k_1(x_1+\tfrac{L_1}{2})\cos k_2(x_2+\tfrac{L_2}{2})\{k_\ell[A_{1N}\sin k_\ell(x_3+\tfrac{L_3}{2})-A_{2N}\cos k_\ell(x_3+\tfrac{L_3}{2})]\\
&\quad + \frac{1}{k_t}[(k_1A_{4N}+k_2A_{6N})\cos k_t(x_3+\tfrac{L_3}{2})-(k_1A_{3N}+k_2A_{5N})\sin k_t(x_3+\tfrac{L_3}{2})]\}\sin\omega_N t\ ,
\end{aligned} \tag{3.4.4}$$

which may then be substituted into the boundary conditions (3.4.1) to obtain the same characteristic equation and amplitude relations as before.

The results for the forced vibration case are developed in like fashion and yield similar results, again the only difference is in the

arguments of the spatial sin and cos terms. Thus, $k_1(x_1+\frac{L_1}{2})$, $k_2(x_2+\frac{L_2}{2})$, $k_\ell(x_3+\frac{L_3}{2})$, and $k_t(x_3+\frac{L_3}{2})$ should be substituted for k_1x_1, k_2x_2, $k_\ell x_3$, and $k_t x_3$, respectively; otherwise, the results are the same.

CHAPTER IV

ELASTICALLY RESTRAINED/RIGID-LUBRICATED BOUNDARIES

4.1 Free and Forced Vibration Solutions

For the free vibration problem, the two stress-free boundaries of Chapter III are replaced by two elastically restrained boundaries, and the four rigid-lubricated boundaries remain unchanged:

$$\begin{array}{lll} x_1 = 0, L_1 & u_1 = 0 & \dfrac{\partial u_2}{\partial x_1} = \dfrac{\partial u_3}{\partial x_1} = 0 \\ x_2 = 0, L_2 & u_2 = 0 & \dfrac{\partial u_1}{\partial x_2} = \dfrac{\partial u_3}{\partial x_2} = 0 \\ x_3 = 0, L_3 & \dfrac{\partial u_1}{\partial x_1} + \dfrac{\partial u_2}{\partial x_2} + \gamma \dfrac{\partial u_3}{\partial x_3} = \pm \dfrac{e_3 u_3}{\lambda} & \dfrac{\partial u_3}{\partial x_1} + \dfrac{\partial u_1}{\partial x_3} = \dfrac{\partial u_3}{\partial x_2} + \dfrac{\partial u_2}{\partial x_3} = 0. \end{array} \tag{4.1.1}$$

Here e_3 is the elastic modulus of the upper and lower restraints and $\gamma = 1 + \frac{2\mu}{\lambda}$. As before, the free vibration equation of motion is

$$c_t^2 \nabla^2 \bar{u} + (c_\ell^2 - c_t^2) \nabla\nabla \cdot \bar{u} = \frac{\partial^2 \bar{u}}{\partial t^2} . \tag{4.12}$$

The development of the normal mode displacement components is the same as that in Chapter III, and as such, only the results are presented here:

$$\begin{aligned} u_{1N} &= \sin k_1 x_1 \cos k_2 x_2 [k_1 (A_{1N} \cos k_\ell x_3 + A_{2N} \sin k_\ell x_3) + A_{3N} \cos k_t x_3 + A_{4N} \sin k_t x_3] \sin \omega_N t \\ u_{2N} &= \cos k_1 x_1 \sin k_2 x_2 [k_2 (A_{1N} \cos k_\ell x_3 + A_{2N} \sin k_\ell x_3) + A_{5N} \cos k_t x_3 + A_{6N} \sin k_t x_3] \sin \omega_N t \\ u_{3N} &= \cos k_1 x_1 \cos k_2 x_2 \{k_\ell (A_{1N} \sin k_\ell x_3 - A_{2N} \cos k_\ell x_3) \\ &\quad + \frac{1}{k_t} [(k_1 A_{4N} + k_2 A_{6N}) \cos k_t x_3 - (k_1 A_{3N} + k_2 A_{5N}) \sin k_t x_3] \sin \omega_N t \end{aligned} \tag{4.1.3}$$

These components are then substituted into boundary conditions (4.1.1) with the result that the twelve boundary conditions on the x_1 and x_2 faces are satisfied identically and the remaining six boundary conditions on the x_3 faces are satisfied when

$$\lambda(k_1^2 + k_2^2 + \gamma k_\ell^2)k_t A_{1N} + e_3 k_\ell k_t A_{2N} - 2\mu k_1 k_t A_{3N} - e_3 k_1 A_{4N} - 2\mu k_2 k_t A_{5N} - e_3 k_2 A_{6N} = 0$$

$$\begin{aligned}&[\lambda(k_1^2 + k_2^2 + \gamma k_\ell^2)k_t \cos k_\ell L_3 + e_3 k_\ell k_t \sin k_\ell L_3]A_{1N} \\ &\quad + [\lambda(k_1^2 + k_2^2 + \gamma k_\ell^2)k_t \sin k_\ell L_3 - e_3 k_\ell k_t \cos k_\ell L_3]A_{2N} \\ &- [2\mu k_1 k_t \cos k_t L_3 + e_3 k_1 \sin k_t L_3]A_{3N} - [2\mu k_1 k_t \sin k_t L_3 - e_3 k_1 \cos k_t L_3]A_{4N} \\ &- [2\mu k_2 k_t \cos k_t L_3 + e_3 k_2 \sin k_t L_3]A_{5N} - [2\mu k_2 k_t \sin k_t L_3 - e_3 k_2 \cos k_t L_3]A_{6N} = 0\end{aligned}$$

$$2k_1 k_\ell k_t A_{2N} - (k_1^2 - k_t^2)A_{4N} - k_1 k_2 A_{6N} = 0 \qquad (4.1.4)$$

$$\begin{aligned}&- 2k_1 k_\ell k_t \sin k_\ell L_3 A_{1N} + 2k_1 k_\ell k_t \cos k_\ell L_3 A_{2N} + (k_1^2 - k_t^2)\sin k_t L_3 A_{3N} \\ &\quad - (k_1^2 - k_t^2)\cos k_t L_3 A_{4N} + k_1 k_2 \sin k_t L_3 A_{5N} - k_1 k_2 \cos k_t L_3 A_{6N} = 0\end{aligned}$$

$$2k_2 k_\ell k_t A_{2N} - k_1 k_2 A_{4N} - (k_2^2 - k_t^2)A_{6N} = 0$$

$$\begin{aligned}&- 2k_2 k_\ell k_t \sin k_\ell L_3 A_{1N} + 2k_2 k_\ell k_t \cos k_\ell L_3 A_{2N} + k_1 k_2 \sin k_t L_3 A_{3N} - k_1 k_2 \cos k_1 L_3 A_{4N} \\ &\quad + (k_2^2 - k_t^2)\sin k_t L_3 A_{5N} - (k_2^2 - k_t^2)\cos k_t L_3 A_{6N} = 0.\end{aligned}$$

These expressions are valid for finite values of e_3.

As in Chapter 3, the appropriate amplitude relations and frequency equations are determined from the above equations and depend upon the values of $\sin k_t L_3$ and the wave numbers k_1 and k_2. Table 4.1 lists these combinations. Equations (4.1.5) and (4.1.6) correspond to the SH wave motion and are identical to equations (3.1.20) and (3.1.21) from Table 3.1. The longitudinal wave motion described by equations (4.1.7)

TABLE 4.1. Appropriate Modal Coefficients and Frequency Equations, Elastically Restrained/Rigid-Lubricated Boundaries ($0<e_3<\infty$)

Modal Coefficients	$\sin k_t L_3=0$	$\sin k_t L_3\neq 0$		
	$k_1>0,\ k_2>0$	$k_1=k_2=0$	$k_1>0,\ k_2=0$	$k_1\geq 0,\ k_2=0$
A_{1N}	0	$-\frac{e_3}{\delta}A_{2N}$	$-\frac{P}{R}\left(\frac{k_1^2-k_t^2}{2k_1k_\ell k_t}\right)\left[A_{3N}-\frac{e_3(k_1^2+k_t^2)k_\ell}{R}A_{4N}\right]$	$\left(\frac{k_1^2+k_2^2-k_t^2}{2k_2k_\ell k_t}\right)\left[\frac{\sin k_t L_3}{\sin k_\ell L_3}A_{5N}+\frac{(\cos k_\ell L_3-\cos k_t L_3)}{\sin k_\ell L_3}A_{6N}\right]$
A_{2N}	0	*	$\frac{k_1^2-k_t^2}{2k_1k\,k_t}A_{4N}$	$\frac{k_1^2+k_2^2-k_t^2}{2k_2k_\ell k_t}A_{6N}$
A_{3N}	$-\frac{k_2}{k_1}A_{5N}$	0	$\left[\frac{e_3(k_1^2+k_2^2)k_\ell\sin k_\ell L_3-R(\cos k_\ell L_3-\cos k_t L_3)}{P\sin k_\ell L_3+R\sin k_t L_3}\right]A_{4N}$	$\frac{k_1}{k_2}A_{5N}$
A_{4N}	0	0	*	$\frac{k_1}{k_2}A_{6N}$
A_{5N}	*	0	0	$\frac{e_3(k_1^2+k_2^2+k_t^2)k_\ell\sin k_\ell L_3-R(\cos k_\ell L_3-\cos k_t L_3)}{P\sin k_\ell L_3+R\sin k_t L_3}$
A_{6N}	0	0	0	*
	(4.1.5)	(4.1.7)	(4.1.9)	(4.1.10)
Frequency Equations	$\omega_N=c_t\alpha$	$e_3^2+2e_3\delta\cot k_\ell L_3-\delta^2=0$	$\{e_3^2(k_1^2+k_2^2+k_t^2)^2k_\ell^2\sin k_\ell L_3\sin k_t L_3-2e_3(k_1^2+k_2^2+k_t^2)k_\ell(P\sin k_\ell L_3\cos k_t L_3+R\cos k_\ell L_3\sin k_t L_3)$ $-[(P^2+R^2)\sin k_\ell L_3\sin k_t L_3+2PR(1-\cos k_\ell L_3\cos k_t L_3)]\}\sin k_t L_3=0$	
	(4.1.6)	(4.1.8)	(4.1.11)	
	$\alpha^2=k_1^2+k_2^2+k_3^2$	$\delta=\lambda\gamma k_\ell$	$P=4(k_1^2+k_2^2)k_\ell k_t$ $\quad R=(k_1^2+k_2^2-k_t^2)^2$	

* For the free vibration problem, these values are determined from the initial conditions; in the forced vibration problem, from the forcing function.

and (4.1.8) is similar to that described by equations (3.1.22) and (3.1.23), except more complicated, in that the natural frequencies are now a function of both the elastic modulus e_3 and the wave number k_ℓ, instead of just the latter. Finally, the SV/P motion is given by equations (4.1.9), (4.1.10), and (4.1.11). Here again, the amplitudes denoted by the asterisks are determined from the intial conditions for the free vibration problem or from the forcing function for the forced vibration problem.

A superposition of the displacement due to the wave components traveling in all directions yields the three-dimensional displacement components

$$\begin{aligned} u_1 &= \sum_N u_{1N} \\ u_2 &= \sum_N u_{2N} \\ u_3 &= \sum_N u_{2N} \end{aligned} \tag{4.1.12}$$

with the u_{iN} (i=1,2,3) as given by equations (4.1.3). This completes the free vibration solution for the rectangular parallelepiped with elastically restrained/rigid-lubricated boundaries. The forced vibration solution proceeds exactly as in Section 3.2, and the results are the same.

4.2 Reduction to the Previous Cases

The free and forced vibration solution for the parallelepiped with elastically restrained/rigid-lubricated boundaries is particularly interesting in that by allowing $e_3 \to \infty$, the normal restraints on the x_3 faces become rigid. Thus, all of the boundaries become rigid-lubricated

as in Chapter II, and the same results should be obtained. Conversely, letting $e_3 \to \infty$, the normal stresses acting on the x_3 faces approach zero, and the stress-free solution of Chapter III should be recovered. From the above, it can be seen that the elastically restrained/rigid-lubricated solution can serve as a check on the previous solutions.

We begin by dividing the normal stress boundary conditions on the x_3 faces (4.1.1c) by e_3, and then we let $e_3 \to \infty$. The result is $u_3=0$, which means that the shear stress conditions can be written as $\partial u_1/\partial x_3=\partial u_2/\partial x_3=0$, and the completely rigid-lubricated boundary conditions (2.1.2) have been recovered. The characteristic equations, on the other hand, must be divided by e_3^2 before allowing $e_3 \to \infty$. For the transcendental equation (4.1.11), this gives

$$(k_1^2+k_2^2+k_t^2)^2\, k_\ell^2 \sin k_\ell L_3 \sin k_t L_3 \sin k_t L_3 = 0$$

but since $(k_1^2+k_2^2+k_\ell^2)^2 k_\ell^2 \neq 0$, the frequency equation becomes

$$\sin k_\ell L_3 \sin k_t L_3 \sin k_t L_3 = 0. \tag{4.2.1}$$

The implication here is that either

$$k_\ell = \frac{n\pi}{L_3},$$

$$(k_t)_1 = \frac{n\pi}{L_3}$$

or

$$(k_t)_2 = \frac{n\pi}{L_3} \qquad n=0,1,2,\ldots;$$

but, $k_3 = \dfrac{n_3\pi}{L_3}$ $(n_3=0,1,2,\ldots)$, meaning that

$$k_\ell=(k_t)_1=(k_t)_2=k_3. \tag{4.2.2}$$

However, by definition,

$$k_\ell^2 = \frac{\omega_N^2}{c_\ell^2} - (k_1^2 + k_2^2) \tag{4.2.3}$$

$$k_t^2 = \frac{\omega_N^2}{c_t^2} - (k_1^2 + k_2^2) \tag{4.2.4}$$

and

$$\alpha_N^2 = k_1^2 + k_2^2 + k_3^2 \ . \tag{4.2.5}$$

Combing equations (4.2.2) through (4.2.5), one obtains the frequency equations

$$\omega_{1N} = c_\ell \alpha_N \tag{4.2.6}$$

$$\omega_{2N} = \omega_{3N} = c_t \alpha_N \ , \tag{4.2.7}$$

which are identical to (2.1.6) and (2.1.7), as expected.

The appropriate amplitude relations are recovered by performing a division and limiting operating similar to the above on equations (4.1.4), keeping in mind the relationships given in equation (4.2.2). This procedure leads to the result that

$$A_{2N} = A_{4N} = A_{6N} = 0 \ , \tag{4.2.8}$$

which means that the displacement components of equations (4.1.3) reduce to

$$\begin{aligned}
u_{1N} &= \sin k_1 x_1 \cos k_2 x_2 \cos k_3 x_3 [k_1 A_{1N} \sin\omega_{\ell N} t + A_{3N} \sin\omega_{tN} t] \\
u_{2N} &= \cos k_1 x_1 \sin k_2 x_2 \cos k_3 x_3 [k_2 A_{1N} \sin\omega_{\ell N} t + A_{5N} \sin\omega_{tN} t] \\
u_{3N} &= \cos k_1 x_1 \cos k_2 x_2 \sin k_3 x_3 [k_3 A_{1N} \sin\omega_{\ell N} t - (\frac{k_1}{k_3} A_{3N} + \frac{k_2}{k_3} A_{5N}) \sin\omega_{tN} t].
\end{aligned} \tag{4.2.9}$$

If we let $k_1 A_{1N} = (A_{1N})_\ell$, $A_{3N} = (A_{1N})_t$, and $A_{5N} = (A_{2N})_t$ and add up all the normal modes, the displacements obtained are the same as those obtained in Chapter II, equations (2.1.11):

$$
\begin{aligned}
u_1 &= \sum_N \sin k_1 x_1 \cos k_2 x_2 \cos k_3 x_3 \{(A_{1N})_\ell \sin\omega_{\ell N} t + (A_{1N})_t \sin\omega_{tN} t\} \\
u_2 &= \sum_N \cos k_1 x_1 \sin k_2 x_2 \cos k_3 x_3 \{\frac{k_2}{k_1}(A_{1N})_\ell \sin\omega_{\ell N} t + (A_{2N})_t \sin\omega_{tN} t\} \qquad (4.2.10) \\
u_3 &= \sum_N \cos k_1 x_1 \cos k_2 x_2 \sin k_3 x_3 \{\frac{k_3}{k_1}(A_{1N})_\ell \sin\omega_{\ell N} t - [\frac{k_1}{k_3}(A_{1N})_t + \frac{k_2}{k_3}(A_{2N})_t]\sin\omega_{tN} t\}.
\end{aligned}
$$

Therefore, allowing the elastic modulus of the boundary restraint on the two x_3 faces to become infinitely large eliminates any displacements normal to these surfaces, and the boundary conditions become completely rigid-lubricated.

Substitution of $e_3 \to 0$ into equations (4.1.1), (4.1.4), and the equations of Table 4.1 yields equations (3.1.2), (3.1.19) and the equations of Table 3.1. Hence, when the elastic modulus of the restraint on the x_3 faces approaches zero, the boundaries become stress-free, and the complete stress-free/rigid-lubricated solution of Chapter III is recovered.

CHAPTER V

RESULTS AND CONCLUSIONS

5.1 Numerical Results

Numerical results were computed for the response of a parallelepiped with stress-free/rigid-lubricated boundaries to an impulsive body force (c.f. Section 3.3 and Appendices B and C). Since the infinite series solutions of equations (3.3.4) had to be truncated and a displacement vs. time curve was the desired result, it was decided that the truncation should be performed so as to include all the resonant frequencies from DC to some cutoff frequency f_{co}. The specimen was a .0254 x .0254 x .0254 m (1 x 1 x 1 in.) aluminum (ρ=2700 kg/m^3) block. The two cutoff frequencies chosen were 1.25 MHz and 2.0 MHz.

It was found that the first eleven wave numbers had to be considered in order to include all the normal modes with natural frequencies up to 1.25 MHz. Thus, the normal mode indices $N(n_1,n_2,n_3)$ varied from $N(0,0,n_3)$ to $N(10,10,n_3)$. Associated with these indices were 480 frequencies (modes) which produced significant displacements in the x_3 direction. The 2.0 MHz cutoff frequency required the inclusion of the first seventeen wave numbers in the x_1 and x_2 directions. This resulted in 1574 contributing modes.

Figure 5.1 shows the u_3 displacement vs. time history at the position .0127, .0127, .0147 m due to a 1 N-sec Dirac delta function

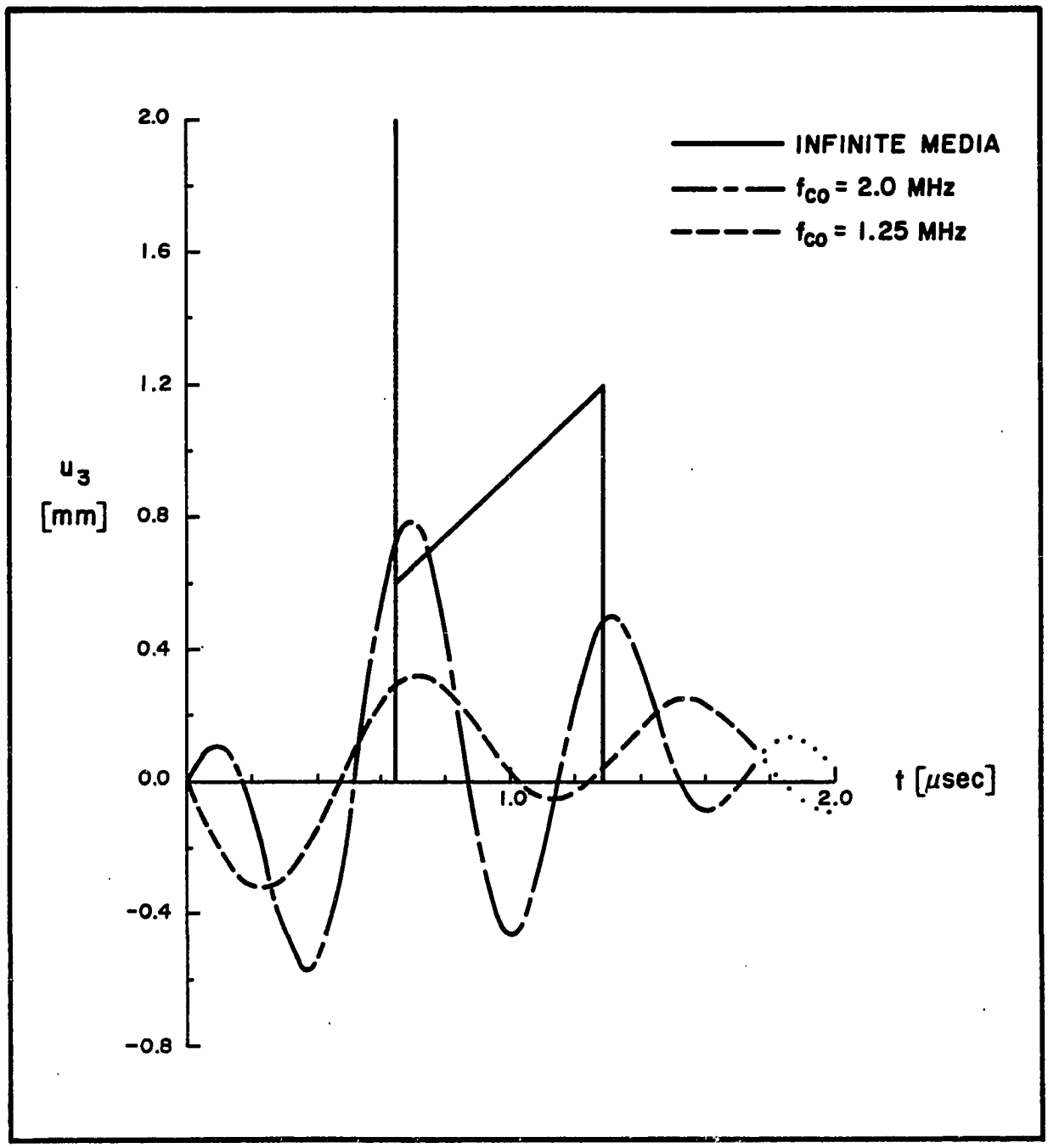

FIGURE 5.1

RESPONSE OF A RECTANGULAR PARALLELEPIPED WITH TWO STRESS-FREE AND FOUR RIGID-LUBRICATED FACES TO AN IMPULSIVE POINT LOAD — TRUNCATED NORMAL MODE SOLUTIONS — COMPARED TO THE INFINITE MEDIA RESPONSE

impulse acting in the x_3 direction at .0127, .0127, .0107 m. Since the first 1.74 μsec of time history is reflection free, this part of the solution may be compared to the exact solution for an infinite body subjected to the same loading [24,25]. This solution consists of an infinite spike corresponding to the arrival of the longitudinal wave followed by a ramp which drops to zero when the shear wave arrives. The other two curves are truncated normal mode solutions to the parallelepiped problem. The dotted portions of these curves begin at 1.74 μsec, the time at which the first reflection occurs and indicate that these values cannot be compared with the infinite media solution. The f_{co} = 2.0 MHz solution is obviously a better approximation to the infinite media response than is the f_{co} = 1.25 MHz solution, but neither of these truncated solutions does a very good job. More frequencies (normal modes) are needed.

To illustrate this point, consider the frequency spectrum (Fourier transform) of a Dirac delta function impulse. It has a constant amplitude for all frequencies from DC to infinity. This means that all frequency components contribute equally to the computed results. Thus, any truncated representation will obviously contain distortions; the fewer the frequencies, the greater the distortion.

Figure 5.2 shows the inverted Fourier transform of the infinite space solution. It was calculated using a Fast Fourier Transform (FFT) routine which was truncated at 10 MHz. The difference between this solution and the infinite media response is due primarily to the Gibbs phenomenon [26] which manifests itself as a ripple in the output. This phenomenon arises whenever a spectral representation is truncated

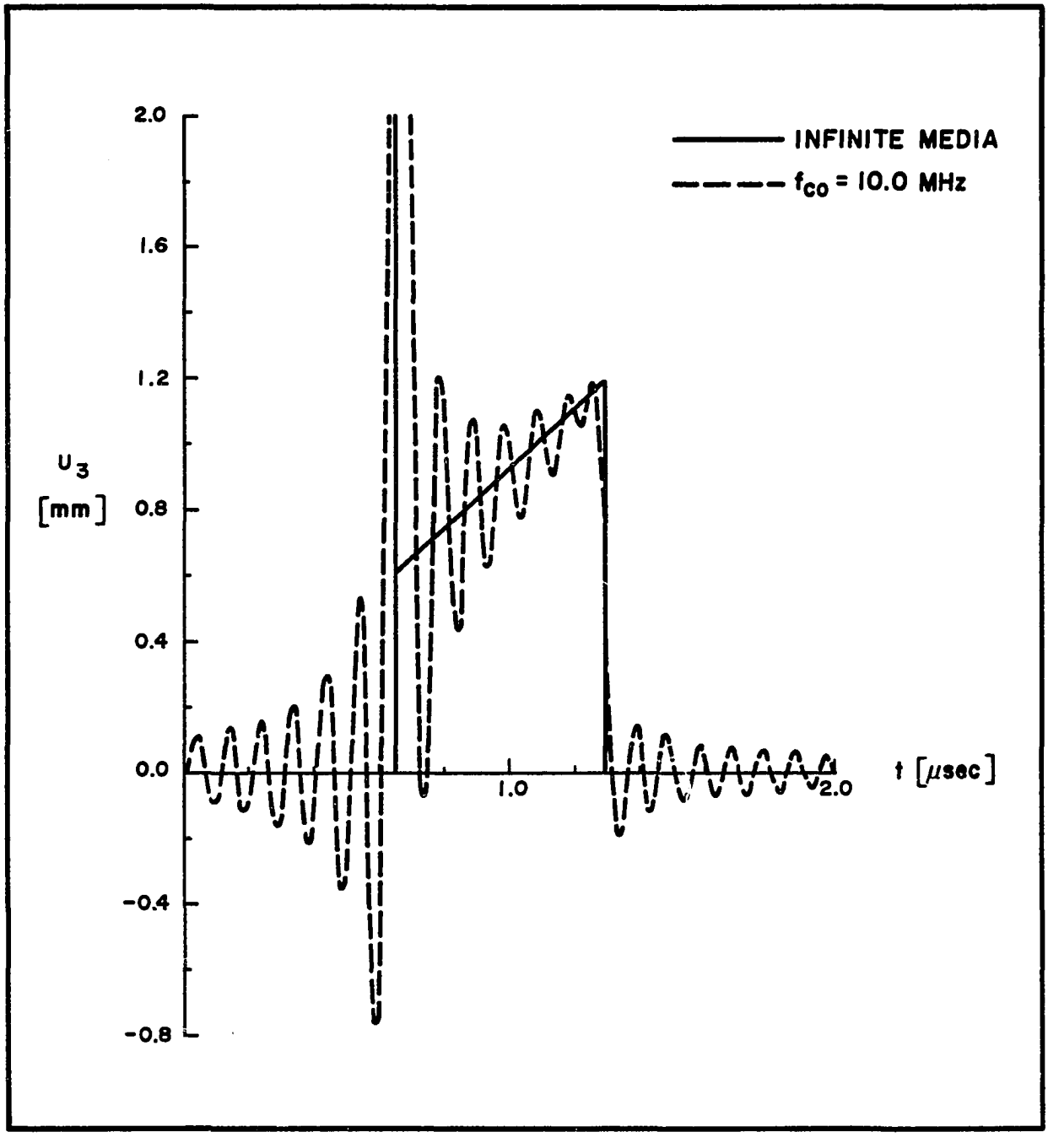

FIGURE 5.2

TRUNCATED FFT REPRESENTATION OF THE INFINITE MEDIA RESPONSE TO AN IMPULSIVE POINT LOAD

abruptly. In this case, the frequencies above 10 MHz are eliminated from consideration. It can be seen from both Figures 5.1 and 5.2 that the ripple frequency is roughly equal to the cutoff frequency f_{co}.

In numerical computations such as this, where infinite series are involved, the accuracy of the final output is obviously limited by the available CPU time. This is compounded by the fact that the transcendental frequency equations (those involving mode conversions) must be solved iteratively. For the 1.25 MHz cutoff frequency, the CPU time required was 9.5 minutes; the 2.0 MHz solution required 32.25 minutes. The majority of this time was taken in solving for the natural frequencies. The larger the specimen, the more resonant frequencies there are to find. In spite of these limitations, the results seem to be headed in the right direction.

A similar analysis was performed by Hill and Egle [20] for the rectangular parallelepiped with completely rigid-lubricated boundaries. The nearly 2600 contributing modes (out of the 2×10^5 considered) were solved for explicitly from the two rather simple frequency equations, $\omega_N = c_\ell \alpha$ and $\omega_N = c_t \alpha$, (2.1.6) and (2.1.7). Because they could be solved for explicitly, rather than implicitly, far more natural frequencies were considered. The additional frequencies improved the accuracy to the point where the normal mode solution and the truncated FFT solution were virtually identical.

5.2 Conclusions and Future Directions

Presented here are exact normal mode solutions for the forced vibrational response of the rectangular parallelepiped with three sets of boundary conditions: (1) completely rigid-lubricated boundaries;

(2) two stress-free and four rigid-lubricated boundaries; and (3) two elastically restrained and four rigid-lubricated boundaries. For cases (1) and (2), the response is calculated for a Dirac delta function impulsive body force. An analytical verification for both solutions is obtained from the elastically restrained solution.

By allowing the elastic modulus of the restraint e_3 to approach infinity, the completely rigid-lubricated results are obtained. When the elastic modulus is allowed to approach zero, the stress-free/rigid-lubricated solution is recovered. The fact that these reductions can be made indicates that these solutions are probably correct, and although not as conclusive in the stress-free/rigid-lubricated case, the numerical results tend to reinforce this conclusion.

The forced vibration solution for the rectangular parallelepiped with completely rigid-lubricated boundaries might be used to model the vibration of a lubricated rubber block completely enclosed in a rigid metal container and stimulated by some internal source. In this case, the normal displacements at the surface are negligible; as a result, there are no mode conversions and hence no inhomogeneous (surface) waves. Though not a physically commonplace problem, the chief value of this solution is the insight it provides into solving the more difficult stress-free and elastically restrained cases.

The stress-free/rigid-lubricated solution, on the other hand, if programmed on a state-of-the-art scientific computer, could prove to be very useful in studying fracture mechanics, and in particular, acoustic emission source events. The elastically restrained/rigid-lubricated solution might be even better in this regard. Both solutions allow for

mode conversions on two of the six faces, and both therefore take into account all three major wave types — shear, longitudinal and surface waves — which provides a better model for the typical acoustic emission application.

All three solutions were developed on the premise that acoustic emission is primarily a body force phenomenon. Although this is true, acoustic emission is more conveniently simulated on the surface of a specimen. If the equation of motion was modified to include surface forces [22] and the length dimensions L_1 and L_2 were allowed to become very large in comparison to L_3, the above solutions could be compared to the work on simulated acoustic emission in plates by Pardee and Graham [2] and Hsu, Simmons and Hardy [2]. Such a formulation would also lend itself better to experimental verification since surface forces of known location are easily generated, whereas body forces are neither easy to generate nor to locate. Including the surface forces would also allow the weight of the transducer to be modeled.

The ultimate goal is to completely bridge the gap between the experimental and analytical, such that flaw growth in structural materials can be predicted and, perhaps to some extent, controlled. The forced vibration solution for the rectangular parallelepiped with completely stress-free boundaries would be a significant step in this direction. Unfortunately, none of the three solutions could be extended by superposition to attain the completely stress-free solution. In each instance, the twelve shear stress boundary conditions were satisfied but not the six normal stress conditions. However, the three solutions presented here do represent a meaningful contribution to the field.

With the inclusion of surface forces, these solutions could very well provide a means of extending Hatano's Rayleigh wave calibration of piezoelectric transducers [26] to include all three wave types. They might also serve to verify the diffuse field calibration technique [27]. In conclusion, if these three solutions do nothing else, they will have at least broadened the author's horizons.

REFERENCES

1. Pardee, W.J. and Graham, L.J., "Frequency Analysis of Two Types of Simulated Acoustic Emissions", Journal of the Acoustical Society of America, Vol. 63, No. 3, March 1978, pp. 793-799.

2. Hsu, N.N., Simmons, J.A., and Hardy, S.C., "An Approach to Acoustic Emission Signal Analysis - Theory and Experiment", Materials Evaluation, Vol. 35, No. 10, October 1977, pp. 100-106.

3. Pao, Y.H., Gajewski, R.R., and Ceranoglu, A.N., "Acoustic Emission and Transient Waves in an Elastic Plate", Journal of the Acoustical Society of America, Vol. 65, No. 1, January 1979, pp. 96-105.

4. Ortway, R., "Uber die Abzählung der Eigenschwingungen fester Körper", Annalen der Physik, Ser. 4, Vol. 42, 1913, pp. 745-760.

5. Nadeau, G., Introduction to Elasticity, Holt, Rinehart and Winston, Inc., New York, 1964, pp. 271-274.

6. Mullick, A.B., "Vibration of a Rectangular Parallelepiped of an Orthotropic Elastic Solid", Bulletin of the Calcutta Mathematical Society, Vol. 62, No. 1, 1970, pp. 35-40.

7. Egle, D.M., "On Estimating the Power of Acoustic Emission Events", paper presented at Society for Experimental Stress Analysis Spring Meeting, Chicago, IL, May 11-16, 1975.

8. Spanner, J.C., Acoustic Emission Techniques and Applications, Intex Publishing Co., Evanston, Illinois, 1974, pp. 10-35.

9. Houghton, J.R., Townsend, M.A., and Packman, P.F., "Optimal Design and Evaluation Criteria for Acoustic Emission Pulse Signature Analysis", Journal of the Acoustical Society of America, Vol. 61, No. 3, March 1977. pp. 859-871.

10. Boresi, A.P. and Lynn, P.P., Elasticity in Engineering Mechanics, Prentice-Hall, Englewood Cliffs, N.J., 1974, pp. 195-196.

11. Graff, K.F., Wave Motion in Elastic Solids, Ohio State University Press, Columbus, Ohio, 1975.

12. Malecki, I., Physical Foundations of Technical Acoustics, Pergamon

Press, New York, 1969, pp. 595-599.

13. Kaliski, S., Pewne Problemy Brzegowe Dynamicznej Teorii Sprezystości i Cial Niesprezystych, Warszawa, 1957.

14. Fromme, J.A., "Vibration of the Rectangular Parallelepiped with Traction Free Boundary", PhD dissertation,Ohio State University, 1967.

15. Fromme, J.A. and Leissa, A.W., "Free Vibration of the Rectangular Parallelepiped", Journal of the Acoustical Society of America, Vol. 48, No. 1 (Part 2), July 1970, pp. 290-298.

16. Budanov, S.P. and Orlov, B.I., "Natural Oscillations of a Rectangular Parallelepiped", Journal of Applied Math & Mechanics (P.M.M.), Vol. 41, No. 1, 1977, pp. 148-152.

17. Kaliski, S., "The Dynamical Problem of the Rectangular Parallelepiped", Archiwum Mechaniki Stosowanej, Vol. 10, 1958, pp. 329-370.

18. Papkovich, P.F., "Solution generale des équations différentielles fundamentales d'élasticité exprimée par trois fonctions harmoniques", Comptes Rendus de l'académie des sciences, Vol. 195, 1932, pp. 513-515 and erratum p. 836.

19. Stephens, R.W.B. and Pollock, A.A., "Waveforms and Frequency Spectra of Acoustic Emissions", Journal of the Acoustical Society of America, Vol. 50, No. 3 (Part 2), September 1971, pp. 904-910.

20. Hill, E.v.K. and Egle, D.M., "Forced Vibrational Response of a Rectangular Parallelepiped with Rigid-Lubricated Boundaries", submitted for publication.

21. Morse, P. and Feshbach, H., Methods of Theoretical Physics, Vol. 1, McGraw-Hill, New York, 1953, pp. 52-53.

22. Pilkey, W., "Dynamic Response of Elastic Bodies Using the Reciprocal Theorem", Journal of Applied Mechanics, Vol. 34, Transactions of the ASME, Vol. 89E, No. 3, September 1967, pp. 774-775.

23. Meirovitch, L., Analytical Methods in Vibrations, Macmillan Co., New York, 1967, pp. 138-143.

24. Achenbach, J.D., Elastic Waves in Solids, North-Holland Publishing Co., Amsterdam, 1973, p. 96-100.

25. Rabiner, L.R. and Gold, B., Theory and Application of Digital Signal Processing, Prentice-Hall, Englewood Cliffs, N.J., 1975, p. 88-101.

26. Hatano, H. and Mori, E., "Acoustic-Emission Transducer and its

Absolute Calibration", Journal of the Acoustical Society of America, Vol. 59, No. 2, February 1976, pp. 344-349.

27. Hill, E.v.K. and Egle, D.M., "A Reciprocity Technique for Estimating the Diffuse-Field Sensitivity of Piezoelectric Transducers", Journal of the Acoustical Society of America, Vol. 67, No. 2, February 1980, pp. 666-672.

BIBLIOGRAPHY

Abramowitz, M. and Stegun, I.A., Handbook of Mathematical Functions, Applied Mathematics Series 55, National Bureau of Standards, Washington, D.C., 1972.

Biezeno, C.B. and Grammel, R., Engineering Dynamics, Vol. I, Theory of Elasticity, Analytical and Experimental Methods, Blackie & Son Ltd., London, 1955.

Carrier, G.F. and Pearson, C.E., Partial Differential Equations, Theory and Technique, Academic, New York, 1976.

Churchill, R.V., Operational Mathematics, 3rd Edition, McGaw-Hill, New York, 1972.

Drouillard, T.F., Acoustic Emission, A Bibliography with Abstracts, Plenum, New York, 1979.

Hildebrand, F.B., Advanced Calculus for Applications, Prentice-Hall, Englewood Cliffs, N.J., 1962.

Hildebrand, F.B., Methods of Applied Mathematics, 2nd Edition, Prentice-Hall, Englewood Cliffs, N.J., 1965.

Johnson, D.E. and Johnson, J.R., Mathematical Methods in Engineering and Physics, Ronald, New York, 1965.

Kreyszig, E., Advanced Engineering Mathematics, 3rd Edition, Wiley, New York, 1972.

Meirovitch, L., Elements of Vibration Analysis, McGraw-Hill, New York, 1975.

O'Nan, M., Linear Algebra, Harcourt Brace Jovanovich, New York, 1971.

APPENDICES

APPENDIX A

Separated Wave Equations

The governing equation for wave propagation in solids is Navier's equation, which may be expressed in terms of the longitudinal and transverse wave speeds as

$$c_t^2 \nabla^2 \bar{u} + (c_\ell^2 - c_t^2) \nabla\nabla\cdot\bar{u} + \bar{f} = \frac{\partial^2 \bar{u}}{\partial t^2} \ . \tag{A1}$$

Substituting the Helmholtz resolutions of displacement

$$\bar{u} = \nabla S + \nabla \times \bar{V} \tag{A2}$$

$$\nabla\cdot\bar{V} = 0 \tag{A3}$$

and body force

$$\bar{f} = \nabla f + \nabla \times \bar{F} \tag{A4}$$

$$\nabla\cdot\bar{F} = 0 \tag{A5}$$

into the equations of motion (A1) gives

$$c_t^2 \nabla^2 (\nabla S + \nabla \times \bar{V}) + (c_\ell^2 - c_t^2) \nabla\nabla\cdot(\nabla S + \nabla \times \bar{V}) + (\nabla f + \nabla \times \bar{F}) = \frac{\partial^2}{\partial t^2} (\nabla S + \nabla \times \bar{V}) \tag{A6}$$

But since

$$\nabla^2(\nabla S) = \nabla(\nabla^2 S)$$

$$\nabla\cdot\nabla S = \nabla^2 S$$

and

$$\nabla^2(\nabla \times \bar{V}) = \nabla \times (\nabla^2 \bar{V})$$

$$\nabla\cdot\nabla \times \bar{V} = 0 \ ,$$

equation (A6) may be rewritten as

$$\nabla(c_\ell^2\nabla^2 S + f - \frac{\partial^2 S}{\partial t^2}) + \nabla \times (c_t^2\nabla^2\bar{V} + \bar{F} - \frac{\partial^2\bar{V}}{\partial t^2}) = 0 \tag{A7}$$

This equation is satisfied if each of the terms in parenthesis vanishes. Hence, the three original equations of motion (A1), each of which included both longitudinal and transverse waves, are separated into the four independent equations

$$c_\ell^2\nabla^2 S + f = \frac{\partial^2 S}{\partial t^2} \tag{A8}$$

$$c_t^2\nabla^2\bar{V} + \bar{F} = \frac{\partial^2\bar{V}}{\partial t^2} \, . \tag{A9}$$

Equation (A8) defines the longitudinal wave motion and equation (A9) the transverse wave motion. These are the separated wave equations. Conditions (A3) and (A5) allow a unique determination of the three components of $\bar{u}$ from the four components of S and $\bar{V}$ and the four components of f and $\bar{F}$.

Free Vibration Case

For the free vibration case, the body force terms vanish and the separated wave equations may be rearranged as

$$\nabla^2 S = \frac{1}{c_\ell^2}\frac{\partial^2 S}{\partial t^2} \tag{A10}$$

$$\nabla^2\bar{V} = \frac{1}{c_t^2}\frac{\partial^2\bar{V}}{\partial t^2} \tag{A11}$$

Both wave equations may be solved by separation of variables. The longitudinal wave equation (A10) may be solved by assuming

$$S(x_1,x_2,x_3,t) = W(x_1,x_2,x_3)T(t); \tag{A12}$$

substitution of this expression into equation (A10) yields

$$\frac{\nabla^2 W}{W} = \frac{T''}{c_\ell^2 T} = -\alpha_\ell^2 \tag{A13}$$

from which

$$\nabla^2 W + \alpha_\ell^2 W = 0 \tag{A14}$$

and

$$T'' + c_\ell^2 \alpha_\ell^2 T = 0. \tag{A15}$$

Equation (A14) is known as the Helmholtz equation. Its solution is obtained by substituting into it

$$W = X_1(x_1)X_2(x_2)X_3(x_3) \tag{A16}$$

with the result

$$\frac{X_1''}{X_1} + \frac{X_2''}{X_2} + \frac{X_3''}{X_3} = -\alpha_\ell^2. \tag{A17}$$

Letting

$$\frac{X_1''}{X_1} = -k_1^2 \tag{A18}$$

$$\frac{X_2''}{X_2} = -k_2^2 \tag{A19}$$

gives the third equation

$$\frac{X_3''}{X_3} = -[\alpha_\ell^2 - (k_1^2 + k_2^2)] = -k_\ell^2. \tag{A20}$$

The frequencies may be defined as $\omega_\ell = c_\ell \alpha_\ell$ and $\omega_t = c_t \alpha_t$; hence, the solutions to equations (A15), (A18), (A19), and (A20) are

$$T(t) = A_1 \cos\omega_\ell t + A_2 \sin\omega_\ell t \tag{A21}$$

and

$$X_1(x_1) = B_1 \cos k_1 x_1 + B_2 \sin k_1 x_1 \tag{A22}$$

$$X_2(x_2) = B_3 \cos k_2 x_2 + B_4 \sin k_2 x_2 \tag{A23}$$

$$X_3(x_3) = B_5 \cos k_3 x_3 + B_6 \sin k_3 x_3 \ , \tag{A24}$$

which, along with the initial condition T(0)=0, may be combined according to equations (A12) and (A16) to give

$$S = (C_1\cos k_1 x_1 + C_2\sin k_2 x_2)(C_3\cos k_2 x_2 + C_4\sin k_2 x_2)(C_5\cos k_\ell x_3 + C_6\sin k_\ell x_3)\sin\omega_\ell t, \tag{A25}$$

the general solution for the free vibration scalar potential. The vector potential components are determined analogously:

$$V_1 = (D_1\cos k_1 x_1 + D_2\sin k_1 x_1)(D_3\cos k_2 x_2 + D_4\sin k_2 x_2)(D_5\cos k_t x_3 + D_6\sin k_t x_3)\sin\omega_t t$$

$$V_2 = (E_1\cos k_1 x_1 + E_2\sin k_1 x_1)(E_3\cos k_2 x_2 + E_4\sin k_2 x_2)(E_5\cos k_t x_3 + E_6\sin k_t x_3)\sin\omega_t t$$

$$V_3 = (F_1\cos k_1 x_1 + F_2\sin k_1 x_1)(F_3\cos k_2 x_2 + F_4\sin k_2 x_2)(F_5\cos k_t x_3 + F_6\sin k_t x_3)\sin\omega_t t. \tag{A26}$$

In view of the frequency definitions above, the longitudinal and transverse wave numbers may be written as

$$k_\ell^2 = \frac{\omega_\ell^2}{c_\ell^2} - (k_1^2 + k_2^2) \tag{A27}$$

$$k_t^2 = \frac{\omega_t^2}{c_t^2} - (k_1^2 + k_2^2) \ . \tag{A28}$$

APPENDIX B

Calculating the Generalized Mass Term

The generalized mass term, E_N, given by equation (3.2.11), is expanded here for computational use:

$$E_N = \int_0^{L_1}\int_0^{L_2}\int_0^{L_3} \bar{\phi}_N \cdot \bar{\phi}_N dx_1 dx_2 dx_3; \tag{B1}$$

but $\bar{\phi}_N \cdot \bar{\phi}_N = \phi_{1N}^2 + \phi_{2N}^2 + \phi_{3N}^2$. Consequently, equation (B1) may be rewritten as

$$E_N = E_{1N} + E_{2N} + E_{3N} , \tag{B2}$$

where

$$E_{iN} = \int_0^{L_1}\int_0^{L_2}\int_0^{L_3} \phi_{iN}^2 dx_1 dx_2 dx_3 , \qquad i=1,2,3. \tag{B3}$$

The ϕ_{iN} (i=1,2,3) are the modal functions defined by equations (3.1.14), (3.1.17), and (3.1.18).

Substituting the modal functions into equations (B3) and performing the indicated integrations results in the following expressions:

$$\begin{aligned} E_{1N} = \frac{\eta_1 L_1 L_2}{4} \{ & k_1^2 (A_{1N}^2 \Delta_1 + 2A_{1N}A_{2N}\Delta_2 + A_{2N}^2 \Delta_3) \\ & + 2k_1 [A_{1N}(A_{3N}\Delta_4 + A_{4N}\Delta_5) + A_{2N}(A_{3N}\Delta_6 + A_{4N}\Delta_7)] \\ & + (A_{3N}^2 \Delta_8 + 2A_{3N}A_{4N}\Delta_9 + A_{4N}^2 \Delta_{10})\} \end{aligned} \tag{B4}$$

$$E_{2N} = \frac{\eta_2 L_1 L_2}{4} \{k_2^2(A_{1N}^2\Delta_1 + 2A_{1N}A_{2N}\Delta_2 + A_{2N}^2\Delta_3)$$
$$+ 2k_2[A_{1N}(A_{5N}\Delta_4 + A_{6N}\Delta_5) + A_{2N}(A_{5N}\Delta_6 + A_{6N}\Delta_7)]$$
$$+ (A_{5N}^2\Delta_8 + 2A_{5N}A_{6N}\Delta_9 + A_{6N}^2\Delta_{10})\} \quad \text{(B5)}$$

$$E_{3N} = \frac{\eta_3 L_1 L_2}{4} \{k_\ell^2(A_{1N}^2\Delta_3 + 2A_{1N}A_{2N}\Delta_2 + A_{2N}^2\Delta_1)$$
$$+ \frac{k_\ell}{k_t}[A_{1N}(k_1A_{4N} + k_2A_{6N})\Delta_6 - A_{1N}(k_1A_{3N} + k_2A_{5N})\Delta_7$$
$$- A_{2N}(k_1A_{4N} + k_2A_{6N})\Delta_4 + A_{2N}(k_1A_{3N} + k_2A_{5N})\Delta_5]$$
$$+ \frac{1}{k_t^2}[(k_1A_{4N} + k_2A_{6N})^2\Delta_8 - 2(k_1A_{4N} + k_2A_{6N})(k_1A_{3N} + k_2A_{5N})\Delta_9$$
$$+ (k_1A_{3N} + k_2A_{5N})^2\Delta_{10}]\}. \quad \text{(B6)}$$

Here,

$$\eta_1 = (1 - \delta_{k_1 0})(1 + \delta_{k_2 0}) \quad \text{(B7)}$$

$$\eta_2 = (1 + \delta_{k_1 0})(1 - \delta_{k_2 0}) \quad \text{(B8)}$$

$$\eta_3 = (1 + \delta_{k_1 0})(1 + \delta_{k_2 0}) \ , \quad \text{(B9)}$$

and

$$\Delta_1 = \frac{L_3}{2} + \frac{\sin 2k_\ell L_3}{4k_\ell} \quad \text{(B10)}$$

$$\Delta_2 = \frac{\sin^2 k_\ell L_3}{2k_\ell} \quad \text{(B11)}$$

$$\Delta_3 = \frac{L_3}{2} - \frac{\sin 2k_\ell L_3}{4k_\ell} \quad \text{(B12)}$$

$$\Delta_4 = \frac{\sin(k_\ell - k_t)L_3}{2(k_\ell - k_t)} \quad \text{(B13)}$$

$$\Delta_5 = \frac{1-\cos(k_\ell + k_t)L_3}{2(k_\ell + k_t)} - \frac{1-\cos(k_\ell - k_t)L_3}{2(k_\ell - k_t)} \tag{B14}$$

$$\Delta_6 = \frac{1-\cos(k_\ell - k_t)L_3}{2(k_\ell - k_t)} + \frac{1-\cos(k_\ell + k_t)L_3}{2(k_\ell + k_t)} \tag{B15}$$

$$\Delta_7 = \frac{\sin(k_\ell - k_t)L_3}{2(k_\ell - k_t)} - \frac{\sin(k_\ell + k_t)L_3}{2(k_\ell + k_t)} \tag{B16}$$

$$\Delta_8 = \frac{L_3}{2} + \frac{\sin k_t L_3}{4k_t} \tag{B17}$$

$$\Delta_9 = \frac{\sin^2 k_t L_3}{2k_t} \tag{B18}$$

$$\Delta_{10} = \frac{L_3}{2} - \frac{\sin 2k_t L_3}{4k_t} \quad . \tag{B19}$$

Finally, all of the above may be combined according to equation (B2) to obtain E_N.

APPENDIX C

A COMPUTER PROGRAM FOR CALCULATING THE X_3-AXIS DISPLACEMENT RESPONSE DUE TO AN IMPULSIVE BODY FORCE

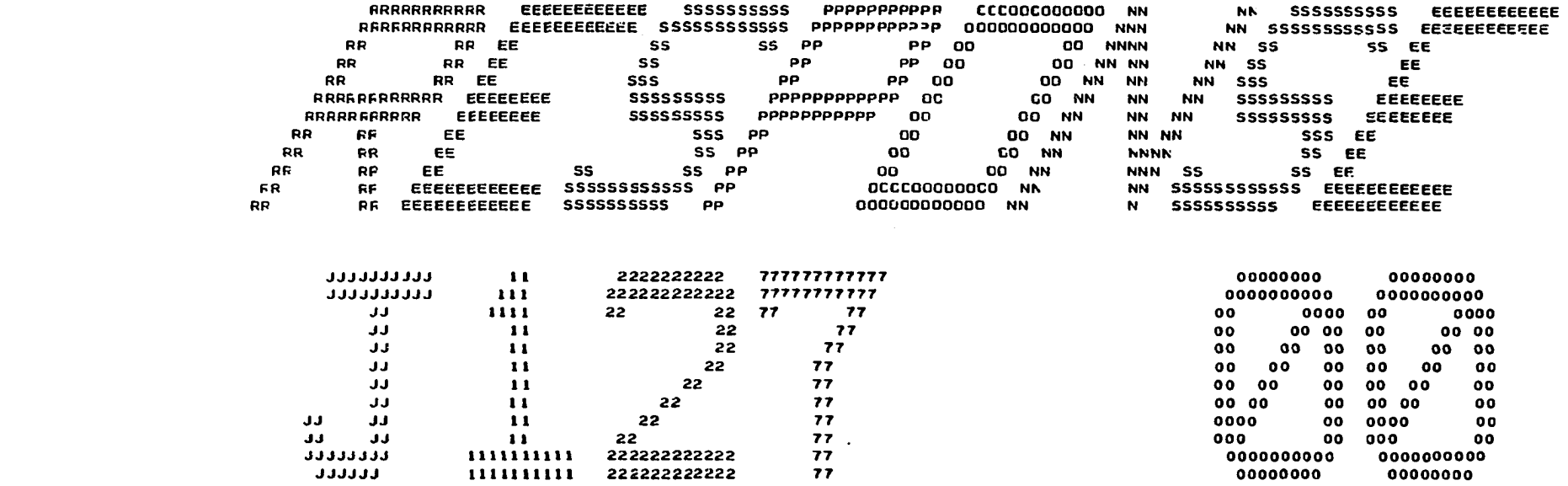


```
POE=RM00,DEST=RM00  START PRT  20.38.41  PRINTER1  80.230  HILL HLD AT MERRICK  (17 AUG 80)  UNIVERSITY OF OKLAHOMA
POE=RM00,DEST=RM00  START PRT  20.38.41  PRINTER1  80.230  HILL HLD AT MERRICK  (17 AUG 80)  UNIVERSITY OF OKLAHOMA
POE=RM00,DEST=RM00  START PRT  20.38.41  PRINTER1  80.230  HILL HLD AT MERRICK  (17 AUG 80)  UNIVERSITY OF OKLAHOMA
POE=RM00,DEST=RM00  START PRT  20.38.41  PRINTER1  80.230  HILL HLD AT MERRICK  (17 AUG 80)  UNIVERSITY OF OKLAHOMA
POE=RM00,DEST=RM00  START PRT  20.38.41  PRINTER1  80.230  HILL HLD AT MERRICK  (17 AUG 80)  UNIVERSITY OF OKLAHOMA
POE=RM00,DEST=RM00  START PRT  20.38.41  PRINTER1  80.230  HILL HLD AT MERRICK  (17 AUG 80)  UNIVERSITY OF OKLAHOMA
```

```
**********************************************************************************
*                                                                                *
*                                                                                *
*                              JES2 NEWS BLOCK                                   *
*                                                                                *
*                                                                                *
*                                                                                *
*                                                                                *
*                                                                                *
*                                                                                *
*                                                                                *
*                                                                                *
*                                                                                *
*                                                                                *
*                                                                                *
*                                                                                *
*                                                                                *
*                                                                                *
*                                                                                *
*                                                                                *
*                                                                                *
**********************************************************************************
```

```
0001                  COMMON XL1,XL2,XL3,XC1,XC2,XC3,CL,WND,IZERO,CT
0002                  COMMON N1,N2,XK1,XK2,X1,X2,X3,ASYMP
0003                  DIMENSION U3(200),U3S(200),FN(15000),D3N(15000)
0004                  COMPLEX A,COEFF,DIFL,DIFT,XKL,XKT,RS,PST,RST,T1,T2,ZER
                  C
                  C     LONGITUDINAL AND TRANSVERSE WAVE SPEEDS
                  C
0005                  CL=6150.
0006                  CT=3100.
                  C
                  C     SPECIMEN DIMENSIONS
                  C
0007                  XL1=.0254
0008                  XL2=.0254
0009                  XL3=.0254
                  C
                  C     POINT OF APPLICATION OF THE IMPULSIVE LOAD
                  C
0010                  XC1=XL1/2.
0011                  XC2=XL2/2.
0012                  XC3=.0107
                  C
                  C     POINT AT WHICH DISPLACEMENTS ARE SENSED
                  C
0013                  X1=XC1
0014                  X2=XC2
0015                  X3=.0147
                  C
                  C     LOWER AND UPPER FREQUENCY BOUNDS
                  C
0016                  PI=3.1415926536
0017                  WNL=(1.0E4)*2.*PI
0018                  WNU=(1.25E6)*2.*PI
                  C
                  C     P AND SV WAVE CHARACTERISTIC FREQUENCIES AND U3 MODAL DISPLACEMENT
                  C     COEFFICIENTS
                  C
0019                  N=1
0020                  ZERO=0.
0021                  IZERO=0
0022                  DELF=250.*PI
0023                  DMIN=1.0E-3
0024                  A=CMPLX(0.,1.)
0025                  ASYMP=18.
0026                  DO 16 J=1,13,2
0027                  N2=J-1
0028                  XN2=N2
0029                  XK2=XN2*PI/XL2
0030                  DO 15 I=1,13,2
0031                  K=1
0032                  L=1
0033                  WN=WNL
0034                  N1=I-1
0035                  XN1=N1
0036                  XK1=XN1*PI/XL1
0037                  WND=XK1*XK1+XK2*XK2
0038                  IF(WND.GT.ZERO) GO TO 2
0039             39   XN3=K
```

```
0040                    WFN=CL*XN3*PI/XL3
0041                    IF(WFN.GT.WNU) GO TO 15
0042                    GO TO 14
0043              2     WFL=WN*WN/(CL*CL)
0044                    WFT=WN*WN/(CT*CT)
0045                    DIFL=WFL-WND
0046                    DIFT=WFT-WND
0047                    XKL=CSQRT(DIFL)
0048                    XKT=CSQRT(DIFT)
0049                    RS=WND-DIFT
0050                    PST=-4.*WND*XKL*XKT
0051                    RST=-RS*RS
0052                    T1=XKL*XL3
0053                    T2=XKT*XL3
0054                    RT1=CABS(T1)
0055                    RT2=CABS(T2)
0056                    COEFF=.5*((PST/RST)+(RST/PST))
0057                    IF(WND.GT.WFL.AND.WND.LT.WFT.AND.RT1.GT.ASYMP) GO TO 40
0058                    IF(WND.GT.WFT.AND.RT2.GT.ASYMP) GO TO 41
0059                    ZER=COEFF*CSIN(T1)*CSIN(T2)+1.-CCOS(T1)*CCOS(T2)
0060                    GO TO 42
0061              40    ZER=A*COEFF*SIN(RT2)-COS(RT2)
0062                    GO TO 42
0063              41    ZER=PST+RST
0064              42    ZR=REAL(ZER)
0065                    ZI=AIMAG(ZER)
0066                    IF(ZR.EQ.ZERO.AND.ZI.EQ.ZERO) GO TO 7
0067                    IF(ZI) 3,20,4
0068              3     KSIGN=1
0069                    GO TO 5
0070              20    KSIGN=2
0071                    GO TO 5
0072              4     KSIGN=3
0073              5     IF(ZR) 6,21,8
0074              6     ISIGN=1
0075                    IF(L-1) 11,11,9
0076              7     WFN=WN
0077                    WN=WN+DELF
0078                    IF(WN.LT.WNU) GO TO 2
0079                    GO TO 15
0080              21    ISIGN=2
0081                    IF(L-1) 11,11,9
0082              8     ISIGN=3
0083                    IF(L-1) 11,11,9
0084              9     IF(JSIGN-ISIGN) 12,10,12
0085              10    IF(LSIGN-KSIGN) 13,11,13
0086              11    OLDWN=WN
0087                    OLDZI=ZI
0088                    OLDZR=ZR
0089                    WN=WN+DELF
0090                    IF(WN.GT.WNU) GO TO 15
0091                    LSIGN=KSIGN
0092                    JSIGN=ISIGN
0093                    L=L+1
0094                    GO TO 2
0095              12    WFN=(ZR*OLDWN-OLDZR*WN)/(ZR-OLDZR)
0096                    CALL FREQ(OLDWN,WN,WFN)
0097                    GO TO 14
```

```
0098            13    WFN=(ZI*OLDWN-OLDZI*WN)/(ZI-OLDZI)
0099                  CALL FREQ(OLDWN,WN,WFN)
0100            14    CALL MDC(WFN,DR)
0101                  ADR=ABS(DR)
0102                  IF(ADR.LT.DMIN) GO TO 58
0103                  WRITE(6,*) I,J,K,WFN,DR,N
0104                  FN(N)=WFN
0105                  D3N(N)=DR
0106                  N=N+1
0107            58    K=K+1
0108                  IF(WND.EQ.ZERO) GO TO 39
0109                  IF(WN.LT.WNU) GO TO 11
0110            15    CONTINUE
0111            16    CONTINUE
0112                  NF=N-1
0113                  PRINT 1
0114            1     FORMAT(1H1)
0115                  WRITE(6,*) NF
0116                  PRINT 1
0117                  DO 18 I=1,NF
0118            18    WRITE(6,63) FN(I),D3N(I)
0119            63    FORMAT(11X,2E20.3)
0120                  PRINT 1
                C
                C     SUMMING THE MODAL DISPLACEMENTS TO DETERMINE THE U3 DISPLACEMENTS
                C     AS A FUNCTION OF TIME
                C
0121                  T=2.0E-8
0122                  F0=3.7037E-4
0123                  DO 61 M=1,200
0124                  U3N=0.
0125                  U3NS=0.
0126                  DO 60 K=1,NF
0127                  DFN=FN(K)
0128                  ARG=DFN*T
0129                  DISP=D3N(K)
0130                  PHI=DISP*SIN(ARG)/DFN
0131                  PHIS=DISP*(1.-COS(ARG))/(DFN*DFN)
0132                  U3N=U3N+F0*PHI
0133                  U3NS=U3NS+F0*PHIS
0134            60    CONTINUE
0135                  U3(M)=U3N
0136                  U3S(M)=U3NS
0137            61    T=T+2.0E-8
0138                  PRINT 1
0139                  WRITE(6,62) (U3(M),M=1,200)
0140            62    FORMAT(11X,5E20.3)
0141                  PRINT 1
0142                  WRITE(6,62) (U3S(M),M=1,200)
0143                  PRINT 1
0144                  STOP
0145                  END
```

```
0001                  SUBROUTINE FREQ(X1,X2,WFN)
0002                  COMMON CL,CT,WND,ASYMP
0003                  COMPLEX DIFL,DIFT,XKL,XKT,RS,PST,RST,T1,T2,COEFF,ZC,A
0004                  A=CMPLX(0.,1.)
0005                  C=WFN
0006                  DO 2 I=1,5
0007                  WFL=C*C/(CL*CL)
0008                  WFT=C*C/(CT*CT)
0009                  DIFL=WFL-WND
0010                  DIFT=WFT-WND
0011                  XKL=CSQRT(DIFL)
0012                  XKT=CSQRT(DIFT)
0013                  RS=WND-DIFT
0014                  PST=-4.*WND*XKL*XKT
0015                  RST=-RS*RS
0016                  T1=XKL*XL3
0017                  T2=XKT*XL3
0018                  RT1=CABS(T1)
0019                  RT2=CABS(T2)
0020                  COEFF=.5*((PST/RST)+(RST/PST))
0021                  IF(WND.GT.WFL.AND.WND.LT.WFT.AND.RT1.GT.ASYMP) GO TO 40
0022                  IF(WND.GT.WFT.AND.RT2.GT.ASYMP) GO TO 41
0023                  ZC=COEFF*CSIN(T1)*CSIN(T2)+1.-CCOS(T1)*CCOS(T2)
0024                  GO TO 42
0025            40    ZC=A*COEFF*SIN(RT2)-COS(RT2)
0026                  GO TO 42
0027            41    ZC=PST+RST
0028            42    ZR=REAL(ZC)
0029                  ZI=AIMAG(ZC)
0030                  IF(ZR) 3,4,5
0031            4     IF(ZI) 3,6,5
0032            3     X1=C
0033                  GO TO 2
0034            5     X2=C
0035            2     C=(X1+X2)/2.
0036            6     WFN=C
0037                  RETURN
0038                  END
```

```
0001                  SUBROUTINE MDC(WFN,DR)
0002                  COMMON XL1,XL2,XL3,XC1,XC2,XC3,CL,WND,IZERO,CT
0003                  COMMON N1,N2,XK1,XK2,X1,X2,X3
0004                  COMPLEX A1,A2,A3,A4,A5,D,DIFL,DIFT,XKL,XKT,RS,PST,RST,T1,T2,DK,SK
0005                  COMPLEX DKL,SKL,TT1,TT2,D1,D2,D3,D4,D5,D6,D7,D8,D9,D10,C1,C2,C3,C4
0006                  COMPLEX AE1,AE2,AE3,BE1,BE2,BE3,Q1,Q2,CE1,CE2,CE3,E1N,E2N,E3N,EN
0007                  COMPLEX P3NX,P3NXC,SX3,SX4,TX3,TX4
0008                  COMPLEX CS1,CS2,CC1,CC2
                      C
                      C     DETERMINATION OF THE MODAL COEFFICIENTS
                      C
0009                  DIFL=(WFN*WFN/(CL*CL))-WND
0010                  DIFT=(WFN*WFN/(CT*CT))-WND
0011                  XKL=CSQRT(DIFL)
0012                  XKT=CSQRT(DIFT)
0013                  RS=WND-DIFT
0014                  PST=-4.*WND*XKL*XKT
0015                  RST=-RS*RS
0016                  T1=XKL*XL3
0017                  T2=XKT*XL3
0018                  CS1=CSIN(T1)
0019                  CS2=CSIN(T2)
0020                  CC1=CCOS(T1)
0021                  CC2=CCOS(T2)
0022               23 IF(N1.GT.IZERO.AND.N2.GT.IZERO) GO TO 30
0023                  IF(N1.EQ.IZERO.AND.N2.GT.IZERO) GO TO 31
0024                  IF(N1.GT.IZERO.AND.N2.EQ.IZERO) GO TO 32
0025                  ETA1=0.
0026                  ETA2=0.
0027                  ETA3=4.
0028                  A6=0.
0029                  A5=CMPLX(0.,0.)
0030                  A4=CMPLX(0.,0.)
0031                  A3=CMPLX(0.,0.)
0032                  A2=CMPLX(1.,0.)
0033                  A1=CMPLX(0.,0.)
0034                  GO TO 34
0035               30 ETA1=1.
0036                  ETA2=1.
0037                  ETA3=1.
0038                  GO TO 33
0039               31 ETA1=0.
0040                  ETA2=2.
0041                  ETA3=2.
0042                  GO TO 33
0043               32 ETA1=2.
0044                  ETA2=0.
0045                  ETA3=2.
0046                  A6=0.
0047                  A5=CMPLX(0.,0.)
0048                  A4=CMPLX(1.,0.)
0049                  A3=-RST*(CC1-CC2)/(PST*CS1+RST*CS2)
0050                  A2=(XK1*XK1-DIFT)/(2.*XK1*XKL*XKT)
0051                  A1=-2.*XK1*A3/(XK1*XK1-DIFT)
0052                  GO TO 34
0053               33 A6=1.
0054                  A5=-RST*(CC1-CC2)/(PST*CS1+RST*CS2)
0055                  A4=XK1/XK2
```

```
0056                A3=A4*A5
0057                A2=RS/(2.*XK2*XKL*XKT)
0058                A1=-A2*A5*PST/RST
                    C
                    C     CALCULATION OF THE GENERALIZED MASS EN.
                    C
0059            34  DK=XKL-XKT
0060                SK=XKL+XKT
0061                DKL=T1-T2.
0062                SKL=T1+T2
0063                D1=(XL3/2.)+CS1*(CC1/(2.*XKL))
0064                D2=CS1*(CS1/(2.*XKL))
0065                D3=(XL3/2.)-CS1*(CC1/(2.*XKL))
0066                C1=CSIN(DKL)/(2.*DK)
0067                C2=CSIN(SKL)/(2.*SK)
0068                C3=(1.-CCOS(SKL))/(2.*SK)
0069                C4=(1.-CCOS(DKL))/(2.*DK)
0070                D4=C1+C2
0071                C5=C3-C4
0072                D6=C3+C4
0073                D7=C1-C2
0074                D8=(XL3/2.)+CS2*(CC2/(2.*XKT))
0075                D9=CS2*(CS2/(2.*XKT))
0076                D10=(XL3/2.)-CS2*(CC2/(2.*XKT))
0077                AE1=A1*A1*D1+2.*A1*A2*D2+A2*A2*D3
0078                AE2=A1*(A3*D4+A4*D5)+A2*(A3*D6+A4*D7)
0079                AE3=A3*A3*D8+2.*A3*A4*D9+A4*A4*D10
0080                BE1=AE1
0081                BE2=A1*(A5*D4+A6*D5)+A2*(A5*D6+A6*D7)
0082                BE3=A5*A5*D8+2.*A5*A6*D9+A6*A6*D10
0083                Q1=XK1*A4+XK2*A6
0084                Q2=XK1*A3+XK2*A5
0085                CE1=A1*A1*D3+2.*A1*A2*D2+A2*A2*D1
0086                CE2=Q1*(A1*D6-A2*D4)+Q2*(A2*D5-A1*D7)
0087                CE3=Q1*Q1*D8-2.*Q1*Q2*D9+Q2*Q2*D10
0088                E1N=XK1*XK1*AE1+2.*XK1*AE2+AE3
0089                E2N=XK2*XK2*BE1+2.*XK2*BE2+BE3
0090                E3N=DIFL*CE1+(XKL*CE2/XKT)+(CE3/DIFT)
0091                EN=(XL1*XL2/4.)*(ETA1*E1N+ETA2*E2N+ETA3*E3N)
                    C
                    C     DETERMINATION OF THE U3 MODAL DISPLACEMENT COEFFICIENTS
                    C
0092                SX1=XK1*X1
0093                SX2=XK2*X2
0094                SX3=XKL*X3
0095                SX4=XKT*X3
0096                P3NX=COS(SX1)*COS(SX2)*(XKL*(A1*CSIN(SX3)-A2*CCOS(SX3))
                   1+(1./XKT)*(Q1*CCOS(SX4)-Q2*CSIN(SX4)))
0097                TX1=XK1*XC1
0098                TX2=XK2*XC2
0099                TX3=XKL*XC3
0100                TX4=XKT*XC3
0101                P3NXC=COS(TX1)*COS(TX2)*(XKL*(A1*CSIN(TX3)-A2*CCOS(TX3))
                   1+(1./XKT)*(Q1*CCOS(TX4)-Q2*CSIN(TX4)))
0102                C=P3NXC*P3NX/EN
0103                DF=REAL(C)
0104            36  RETURN
0105                END
```

-0.436E-04	-0.864E-04	-0.128E-03	-0.166E-03	-0.202E-03
-0.234E-03	-0.262E-03	-0.285E-03	-0.303E-03	-0.316E-03
-0.323E-03	-0.323E-03	-0.319E-03	-0.308E-03	-0.292E-03
-0.271E-03	-0.245E-03	-0.215E-03	-0.182E-03	-0.145E-03
-0.106E-03	-0.651E-04	-0.236E-04	0.182E-04	0.593E-04
0.992E-04	0.137E-03	0.172E-03	0.204E-03	0.233E-03
0.257E-03	0.277E-03	0.292E-03	0.302E-03	0.308E-03
0.309E-03	0.305E-03	0.296E-03	0.284E-03	0.268E-03
0.248E-03	0.226E-03	0.202E-03	0.176E-03	0.149E-03
0.122E-03	0.946E-04	0.684E-04	0.437E-04	0.210E-04
0.614E-06	-0.169E-04	-0.313E-04	-0.422E-04	-0.496E-04
-0.532E-04	-0.532E-04	-0.494E-04	-0.422E-04	-0.317E-04
-0.182E-04	-0.210E-05	0.163E-04	0.364E-04	0.579E-04
0.801E-04	0.103E-03	0.125E-03	0.146E-03	0.167E-03
0.185E-03	0.202E-03	0.216E-03	0.227E-03	0.235E-03
0.241E-03	0.242E-03	0.241E-03	0.236E-03	0.228E-03
0.217E-03	0.203E-03	0.187E-03	0.169E-03	0.149E-03
0.127E-03	0.105E-03	0.821E-04	0.592E-04	0.367E-04
0.151E-04	-0.528E-05	-0.201E-04	-0.409E-04	-0.556E-04
-0.678E-04	-0.774E-04	-0.844E-04	-0.885E-04	-0.900E-04
-0.888E-04	-0.850E-04	-0.789E-04	-0.707E-04	-0.606E-04
-0.490E-04	-0.361E-04	-0.224E-04	-0.825E-05	0.606E-05
0.201E-04	0.336E-04	0.462E-04	0.576E-04	0.675E-04
0.757E-04	0.820E-04	0.864E-04	0.886E-04	0.887E-04
0.868E-04	0.828E-04	0.769E-04	0.693E-04	0.602E-04
0.497E-04	0.382E-04	0.259E-04	0.132E-04	0.282E-06
-0.125E-04	-0.248E-04	-0.364E-04	-0.470E-04	-0.565E-04
-0.645E-04	-0.710E-04	-0.758E-04	-0.788E-04	-0.801E-04
-0.796E-04	-0.774E-04	-0.736E-04	-0.683E-04	-0.617E-04
-0.541E-04	-0.456E-04	-0.365E-04	-0.271E-04	-0.177E-04
-0.860E-05	-0.485E-08	0.779E-05	0.145E-04	0.200E-04
0.240E-04	0.264E-04	0.270E-04	0.258E-04	0.227E-04
0.178E-04	0.111E-04	0.260E-05	-0.744E-05	-0.189E-04
-0.315E-04	-0.451E-04	-0.594E-04	-0.741E-04	-0.889E-04
-0.104E-03	-0.118E-03	-0.131E-03	-0.143E-03	-0.154E-03
-0.164E-03	-0.171E-03	-0.177E-03	-0.180E-03	-0.182E-03
-0.181E-03	-0.178E-03	-0.172E-03	-0.165E-03	-0.155E-03
-0.144E-03	-0.131E-03	-0.117E-03	-0.101E-03	-0.844E-04
-0.673E-04	-0.499E-04	-0.325E-04	-0.155E-04	0.926E-06
0.164E-04	0.307E-04	0.436E-04	0.548E-04	0.642E-04

-0.436E-12	-0.174E-11	-0.388E-11	-0.683E-11	-0.105E-10
-0.149E-10	-0.199E-10	-0.254E-10	-0.312E-10	-0.374E-10
-0.438E-10	-0.503E-10	-0.567E-10	-0.630E-10	-0.690E-10
-0.747E-10	-0.798E-10	-0.845E-10	-0.884E-10	-0.917E-10
-0.942E-10	-0.959E-10	-0.968E-10	-0.969E-10	-0.961E-10
-0.945E-10	-0.921E-10	-0.890E-10	-0.853E-10	-0.809E-10
-0.760E-10	-0.706E-10	-0.649E-10	-0.590E-10	-0.529E-10
-0.467E-10	-0.406E-10	-0.345E-10	-0.287E-10	-0.232E-10
-0.180E-10	-0.133E-10	-0.902E-11	-0.524E-11	-0.200E-11
0.708E-12	0.287E-11	0.450E-11	0.561E-11	0.626E-11
0.647E-11	0.630E-11	0.581E-11	0.507E-11	0.415E-11
0.311E-11	0.204E-11	0.101E-11	0.902E-13	-0.654E-12
-0.116E-11	-0.137E-11	-0.123E-11	-0.703E-12	0.238E-12
0.162E-11	0.344E-11	0.572E-11	0.843E-11	0.116E-10
0.151E-10	0.190E-10	0.231E-10	0.276E-10	0.322E-10
0.370E-10	0.418E-10	0.466E-10	0.514E-10	0.561E-10
0.605E-10	0.647E-10	0.686E-10	0.722E-10	0.754E-10
0.781E-10	0.805E-10	0.823E-10	0.837E-10	0.847E-10
0.852E-10	0.853E-10	0.850E-10	0.844E-10	0.834E-10
0.822E-10	0.807E-10	0.791E-10	0.774E-10	0.756E-10
0.738E-10	0.720E-10	0.704E-10	0.689E-10	0.676E-10
0.665E-10	0.656E-10	0.650E-10	0.647E-10	0.647E-10
0.650E-10	0.655E-10	0.663E-10	0.673E-10	0.686E-10
0.700E-10	0.716E-10	0.733E-10	0.751E-10	0.768E-10
0.786E-10	0.803E-10	0.819E-10	0.834E-10	0.847E-10
0.858E-10	0.866E-10	0.873E-10	0.877E-10	0.878E-10
0.877E-10	0.873E-10	0.867E-10	0.859E-10	0.848E-10
0.836E-10	0.823E-10	0.808E-10	0.792E-10	0.776E-10
0.760E-10	0.745E-10	0.730E-10	0.715E-10	0.702E-10
0.691E-10	0.681E-10	0.673E-10	0.666E-10	0.662E-10
0.659E-10	0.658E-10	0.659E-10	0.661E-10	0.665E-10
0.669E-10	0.674E-10	0.680E-10	0.685E-10	0.690E-10
0.694E-10	0.697E-10	0.698E-10	0.698E-10	0.695E-10
0.690E-10	0.682E-10	0.672E-10	0.659E-10	0.642E-10
0.623E-10	0.601E-10	0.576E-10	0.549E-10	0.519E-10
0.487E-10	0.453E-10	0.419E-10	0.383E-10	0.346E-10
0.310E-10	0.274E-10	0.239E-10	0.205E-10	0.173E-10
0.143E-10	0.116E-10	0.911E-11	0.694E-11	0.509E-11
0.357E-11	0.240E-11	0.157E-11	0.109E-11	0.950E-12
0.113E-11	0.160E-11	0.234E-11	0.333E-11	0.453E-11